Quantum Resistive Behaviors in Vortex Liquid Regimes at Finite Temperatures

Ryusuke Ikeda

Department of Physics, Kyoto University, Kyoto 606-8502

(Received June 7, 2003)

Motivated by a *mean field-like* resistive behavior in magnetic fields commonly seen in various superconducting cuprates and organics with *strong* fluctuation, superconducting (SC) *quantum* fluctuation effects on resistive behaviors are reexamined by putting emphasis on their roles in the so-called *thermal* vortex liquid regime. By incorporating the quantum fluctuations and a vortex pinning effect in the Ginzburg-Landau (GL) fluctuation theory, it is found that the resistivity $\rho(T)$-curve sharply drops, with no fan-shaped broadening, at a vortex-glass transition point far below an *apparent* upper critical field $H_{c2}^*(T)$ as a result of a quantum fluctuation enhanced by an adequately small condensation energy or by a strong field. Fittings to ρ-T data of cuprates and organics are performed by phenomenologically including a SC pseudogap region created by high energy SC fluctuations and possible fluctuations of competing non-SC orders. By examining $\mathrm{La}_{2-x}\mathrm{Sr}_x\mathrm{CuO}_4$ data over a broad doping range, we obtain such conclusions, consistent with recent experimental results, that the in-plane coherence length of hole-doped cuprates decreases with approaching the underdoped limit even in the presence of fluctuating competing orders and that the condensation energy density $(H_c(0))^2 = 0.5[\phi_0/(2\pi\lambda(0)\xi_0)]^2$ is maximal near the optimal doping. Further, the case of disordered quasi 2D films showing the field-tuned superconductor-insulator transition is also examined for comparison and discussed in relation to data reported recently.

KEYWORDS: Quantum Fluctuation, Vortex States, Cuprates, Organic Superconductor

1. Introduction

Macroscopic behaviors in high temperature cuprate superconductors in nonzero magnetic fields ($H \neq 0$) have led to a renewal of our knowledge on the superconducting (SC) fluctuation. In magnetic fields typically of tesla range applied perpendicular to SC layers, both the resistivity $\rho(T, H)$ and heat capacity in some optimally-doped cuprates show a field-induced fan-shaped broadening behavior near and below an *apparent* upper critical field $H_{c2}^*(T)$ to be estimated from thermodynamic quantities. Due to this consistency between ρ and thermodynamic quantities, the resistive broadening was explained as a generic phenomenon in a disordered state (thermal vortex liquid regime) created by the thermal SC fluctuation in nonzero fields.[1–3] After that, the vortex lattice melting transition and its effect on the vanishing of Ohmic resistivity have been studied extensively[4–6] as key issues on the vortex phase diagram in real systems.

However, researches on the vortex phase diagram of cuprates were limited to the case with low enough $H/H_{c2}^*(0)$ values, in which the fluctuation is purely thermal and the vortex pinning effect may be weaker so that the discontinuous nature of the melting transition in pure case may remain intact. The corresponding measurement in higher $H/H_{c2}^*(0)$ values has been realized in overdoped cuprates under several teslas where effects of the pure vortex-solidification are rarely seen. These materials seem to have a longer $T = 0$ in-plane coherence length ξ_0, and their ρ-T curves have shown an apparently mean-field like sharp drop[7, 8] particularly in higher fields. Through a comparison with heat capacity data,[9] however, it is clear at present that the sharp resistivity drop has occurred much below $H_{c2}^*(T)$ (or equivalently, $T_{c2}^*(H)$), possibly except at low enough temperatures, suggesting an enhanced fluctuation effect creating a broad vortex liquid regime in those materials. The data in refs.7 and 9 may be understood by merely assuming a thermal SC fluctuation and noting that the normal conductivity σ_n in the overdoped Tl-compounds[7] is of the order $10^2(R_Q d)^{-1}$: This value is much larger than a typical one of the vortex flow conductivity, i.e., the mean field expression of the superconducting part

$$\sigma_s = \sigma - \sigma_n \tag{1}$$

of the total conductivity σ, so that $\sigma \simeq \sigma_n$ (the normal part of σ) even much below $H_{c2}^*(T)$, where $R_Q = \pi\hbar/2e^2 = 6.45$ (kΩ) is the quantum resistance, and d the distance between the superconducting layers in a layered superconductor. However, such a sharp drop of resistivity much below $H_{c2}^*(T)$ accompanied by a diminishing broadening with increasing field has been also observed in other cuprate superconductors[8, 10–17] and organic superconductors[18, 19] with low $H_{c2}^*(T)$ but with much lower σ_n values ($< 10(R_Q d)^{-1}$) and remains unexplained. Equation (1) implies that σ_s itself is extremely small in the thermal vortex liquid region in the tesla range of these materials.

In this paper, a theory is presented to comprehensively understand such anomalous resistive behaviors in cuprate and organic superconductors with lower $H_{c2}^*(0)$. It is an extension of the previous work[1, 2] to the case with low condensation energy, in which the *quantum* SC fluctuation is not negligible in σ_s in $H \neq 0$ but induces a resistivity curve following the normal (or, quasiparticle) resistivity curve $\rho_n(T) = \sigma_n^{-1}$ even below $H_{c2}^*(T)$. One of our purposes in this paper is to explain how to evaluate intrinsic material parameters of SC materials with strong fluctuation through fittings to resistivity data. Fitting results to data[16] of underdoped La$_{2-x}$Sr$_x$CuO$_4$ (LSCO) based on the present theory were reported in ref.20.

Here, let us briefly explain why the quantum SC fluctuation in the case is important even at *high* temperatures. To do this, it should be first stressed that, in a fixed H, a longer ξ_0 does *not* necessarily imply a weaker fluctuation effect if recalling the fact that the Ginzburg-Landau (GL) fluctuation strength $g_2(H)$ in two dimensional (2D) systems near the zero field

transition temperature T_c is given by[1,6)]

$$g_2(H, T_c) = \frac{16\pi^2 \lambda^2(0) k_{\mathrm{B}} T_c}{\phi_0^2 d} \frac{H}{H_0} \tag{2}$$
$$\propto T_c (\lambda^2(0) \xi_0^2) H,$$

where ϕ_0 is the flux quantum, $\lambda(0)$ is the magnetic penetration depth in $T \to 0$ limit (defined by extraporating from the GL region), and $H_0 \equiv \phi_0/(2\pi\xi_0^2)$ is the *mean field* upper critical field at $T = 0$ defined at the microscopic level. A relation between H_0 and $H_{c2}^*(0)$ will be given in the following sections. According to eq.(2), an increase of ξ_0 under fixed values of other material parameters suggests an enhanced fluctuation at a fixed $H \neq 0$. Note that, in the ordinary 2D GL theory, the Ginzburg number in $H = 0$[5)] is independent of ξ_0 and given by $T_c[\lambda(0)]^2/(\phi_0^2 d)$, except a constant prefactor, which in cuprates decreases monotonically with overdoping. As emphasized elsewhere,[21)] an increase of g_2 leads to an enhancement not only of the thermal fluctuation but of the *quantum* one. In contrast to the $H = 0$ case, the SC fluctuation in $H \neq 0$ remains massive[21)] even deep in the vortex liquid region, and thus, its quantum contribution may play an essential role there. In Fig.1, roles of quantum SC fluctuation in the resistivity are illustrated (Details of calculation leading to Fig.1 will be explained later). Figure 1 (a) also includes a comparison with optimally-doped YBCO data.[22)] If the *quantum* SC fluctuation is taken into account in addition to the thermal one, as the curves in Fig.1 show, an increase of g_2 (in this case, of $\lambda(0)$) results in a more sharp drop of ρ-T curves just above a 3D vortex-glass (VG) transition[4,5)] lying much below $T_{c2}^*(H)$. Throughout this paper, a filled circle on each $\rho(T)$-curve indicates $T_{c2}^*(H)$. The sharp drop of ρ in Fig.1 (b) is a contrast to the fan-shaped broadening around H_{c2}^* in the case Fig.1 (a) dominated by the thermal SC fluctuation[1,5)] and is a consequence of a combination of a (pinning-induced) 3D vortex glass transition and a *reduction* of σ_s brought by the quantum fluctuations in the *thermal* vortex liquid regime.

It has been often argued so far[5)] in relation to the fluctuation effects in cuprates that the SC fluctuation in bulk materials with a large Ginzburg number near T_c and in $H \neq 0$ will be well described as the thermal fluctuation in the 3D XY model. Based on the above-mentioned fact, this conventional picture is invalid. The SC fluctuation in the limit of strong fluctuation is dominated in $H \neq 0$ by its quantum fluctuation contribution. Then, the resistance follows the normal resistance curve even below $H_{c2}^*(T)$ *without* the fan-shaped broadening and shows a mean field-like sudden drop at a VG transition induced by a vortex pinning much below $H_{c2}^*(T)$.

The above-mentioned reduction of σ_s in the thermal vortex liquid regime is due to the same origin as the insulating $\sigma_s(T)$ in the *quantum* vortex liquid regime near $T = 0$.[21,23)] However, in the temperature range where a pinning-induced VG fluctuation effect is negligible, a nearly classical (vortex flow-like) behavior intervenes these two quantum behaviors so that
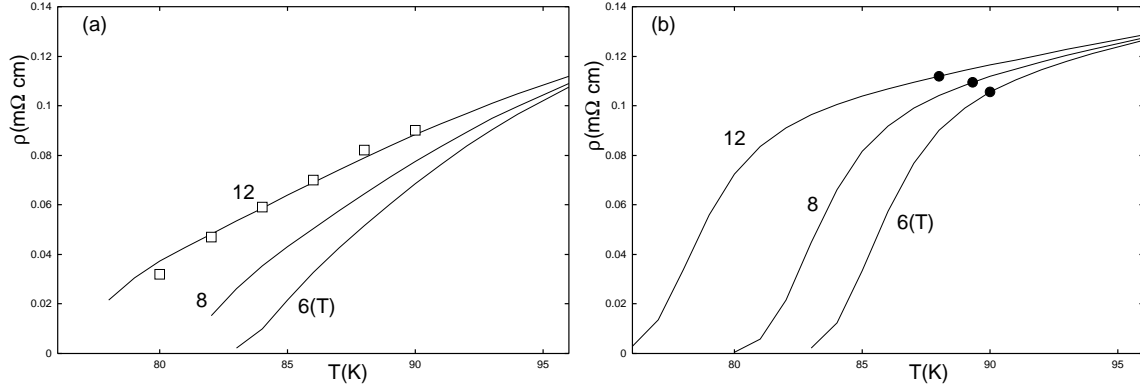
Fig. 1. (a) Resistivity curves (solid lines) in 4, 8, and 12(T) calculated in terms of $\lambda(0) = 0.11(\mu m)$ and 12 (T) data (symbols) in twinned optimally-doped YBCO.[22] See §3 for the details of calculations and other parameter values used here. (b) Same curves as those in (a) except the use of $\lambda(0) = 0.35(\mu m)$. Each darked circle on a $\rho(T)$ curve denotes $T_{c2}^*(H)$ in each H.

they can be conveniently seen as independent ones. In fact, the latter, i.e., a reduction of σ_s near $T = 0$, is limited in most cases to a very low temperature $(T/T_c \ll 1)$ window (see Fig.11 below) and is essential to understanding the field-tuned superconductor-insulator transition (FSIT) behavior[23] which cannot occur without quantum SC fluctuation. Further, thermodynamic quantities such as the magnetization at such low T rapidly vary near $H_{c2}^*(0)$ with sweeping H, reflecting a rise[21] of dimensionality of fluctuation on approaching $T = 0$. In contrast, the reduction of σ_s, i.e., the flatterning of resistance, in the thermal regime appears, as the example of Fig.1 shows, even at high temperatures comparable with T_c in systems with moderately strong fluctuation, and the corresponding T-dependence of thermodynamic quantities is broadened as the quantum fluctuation is stronger (see Figs.8 and 9 below).

Roles of quantum fluctuation of vortex positions in a perfectly clean vortex solid have been examined by Blatter and Ivlev[24] as an explanation of high field behaviors of the first order melting line of a clean vortex solid in optimally-doped YBCO. Note that the fluctuation of vortex positions is included in SC fluctuations because the vortex positions are nodes (zero points) of the SC order parameter. However, it is well understood that the quantum effect on the melting transition of the optimally-doped samples is usually negligible. For instance, an observed field-induced deviation (reduction) of the melting line from the low field behavior is quite small and can be understood rather as a consequence of pinning disorder which is more effective with increasing fields.[4] On the other hand, the quantum fluctuation effect in the thermal vortex liquid regime has not been examined there.[24] Since the fluctuation with lower energy becomes more important upon cooling in the thermal vortex liquid regime (i.e., the disordered non SC phase), it is clear that the quantum fluctuation is much more important, e.g., near $H_{c2}^*(T)$ rather than near the melting line. As Fig.1 (a) shows, however, the quantum

effect on the resistivity curves, and hence, on the melting transition line, of optimally-doped YBCO is quite negligible. When examining in this paper resistivity curves suggestive of a remarkable quantum fluctuation effect, a corresponding quantum effect on a VG transition line replacing the quantum melting line[21] in clean limit is relatively negligible and will not be examined theoretically.

This paper is organized as follows. First, in §2, a semi-quantitative theory describing transport phenomena in the thermal and quantum vortex liquid regimes of 2D-like systems is given. Results in §2 are used in the ensuing sections by incorporating microscopic details to examine data on superconducting cuprates[20] (§3) and organics[25] (§4), and it is shown that the rapid vanishing of resistivity, often seen in these materials, is a consequence of a competition between a strong quantum SC fluctuation and a 3D VG fluctuation. For comparison, resistivity curves in disordered quasi 2D systems with s-wave pairing are also discussed in §5, and it is emphasized through Fig.13 that the rapid vanishing of resistivity much below $H_{c2}^*(T)$ cannot be peculiar to the strongly-correlated electron systems. In addition to data analysis in nonzero fields, effects of the SC pseudogap width and the quantum fluctuation on the critical region near T_c in $H = 0$ are also considered in §6 and an appendix. These two ingredients are expected to be the origins of the unexpectedly[26] narrow $H = 0$ critical region in underdoped cuprates.

In contrast to the dc electric conductivities and the Nernst coefficient, any SC fluctuation effect in a nonsuperconducting (non-SC) phase does not appear, at least in the GL approach, in the thermal conductivity.[27] The latter type of quantities are dominated by a quasiparticle transport[28] even much below H_0. In this paper, we focus primarily on the SC contributions of the former ones and assume their quasiparticle contributions (such as σ_n) to be estimated from experimental data. Since a strong quantum fluctuation deviates σ_s from its mean field vortex flow expression σ_{MF}, we do not expect a possible change of σ_{MF} arising from the gap nodes in unconventional superconductors to lead to a serious discrepancy in our results. Actually, the resistivity defined from the microwave surface impedance data[29] is usually remarkably different from dc resistivity data and is rather comparable with σ_{MF} derived on a single vortex level.

2. Expression of Transport Quantities

In this section, theoretical expressions useful in examining and fitting experimental data of the resistivity ρ and the Nernst coefficient N (or, the transport entropy s_ϕ) are derived. Although the basic framework of the theory is essentially the same as that given in ref.23, we need here to reexpress it in a form applicable to superconductors other than the s-wave dirty films considered there. Our method of renormalization of the SC fluctuation is essentially an extension of the Hartree approximation[1,30] to the case with quantum fluctuation and a vortex pinning effect. Readers who are not interested in the details of derivation of the theoretical

results may skip the main part of this section and jump to the final paragraph of this section.

We start with a 2D GL action

$$S \;\;=\;\; d \int d^2r \left[\beta \sum_\omega (\psi_\omega(\mathbf{r}))^* \gamma(\mathbf{Q}^2) |\omega| \psi_\omega(\mathbf{r}) \right. \tag{3}$$

$$\left. + \;\; \int_0^\beta d\tau \left(u(\mathbf{r})|\psi(\mathbf{r},\tau)|^2 + (\psi(\mathbf{r},\tau))^* \mu(\mathbf{Q}^2)\psi(\mathbf{r},\tau) + \frac{b}{2}|\psi(\mathbf{r},\tau)|^4 \right) \right],$$

as a model of a 2D-like layered superconductor under a field $\mathbf{H}$ perpendicular to the layers. Here, $\mathbf{Q} = -i\nabla + (2\pi/\phi_0)\mathbf{A}(\mathbf{r})$ is the 2D gauge-invariant gradient, $\psi(\tau) = \sum_\omega \psi_\omega e^{-i\omega\tau}$ is a single componet pair-field (SC order parameter), β the inverse temperature, $\omega = 2\pi n/\beta$ with integer n, τ the imaginary time, and $b > 0$. The random potential $u(\mathbf{r})$ has zero mean and satisfies $\overline{u(\mathbf{r})\,u(\mathbf{r}')} = b_p(\mathbf{r} - \mathbf{r}')$. Although the nonlocality of $b_p(\mathbf{r})$ is not negligible in $T \to 0$ limit,[23] we assume that $b_p(\mathbf{r})$ can be replaced hereafter by $\delta(\mathbf{r})$ multiplied by a coefficient b_p because no fluctuation effects close to zero temperature are considered in this paper. Further, the 3D nature due to a coupling between the SC layers was neglected in writing eq.(3) by assuming a strong anisotropy. This assumption is based on the fact found through the previous data fittings[1, 2] that, as far as the vortex pinning is ineffective, the effect of the layer coupling on the *in-plane* electric conductivities in 2D-like systems is extremely weak even deep in the liquid regime. Hence, the 3D nature will be incorporated later in considering a VG contribution to the conductivity. An additional dynamical term $i\gamma'\omega[\psi_\omega]^*\psi_\omega$ leading to a fluctuation Hall effect and resulting from a particle-hole assymmetry was neglected in eq.(3). This is justified as far as $|\gamma'| \ll \gamma$.

When the GL approach is applied to the low T and high H region in which any phase-only approach is inapplicable, H-dependences of the coefficients γ, μ, and b need to be taken into account since the familiar low T divergences[31] of these coefficients in zero field are cut off by the orbital depairing effect of the magnetic field. Thus, their $\mathbf{Q}$-dependences should not be treated perturbatively. Although, strictly speaking, the Pauli paramagnetic depairing effect will also suppress the low T divergences, it will be assumed that it becomes important only in much higher fields than the field range which is focused on in the present work. Then, by expanding ψ in terms of the Landau levels (LLs), $\psi(\mathbf{r}) = \sum_n \varphi_{n,p} u_{n,p}(\mathbf{r})$, the coefficients γ and μ of quadratic terms of eq.(3) are represented as n-dependent ones, μ_n and γ_n, where n (≥ 0) is the LL index, p is a quantum number measuring the degeneracy in each LL, and u_{np} is an eigenfunction in n-th LL. For instance, the *bare* fluctuation propagator $\mathcal{G}_n^{(0)}(|\omega|) = < |\varphi_{n,p}(\omega)|^2 >$ valid in the $b, b_p \to 0$ limit is expressed by $\mathcal{G}_n^{(0)}(|\omega|) = (\gamma_n|\omega|+\mu_n)^{-1}$, where the triangular bracket denotes the ensemble average on ψ. The microscopic mean field transition point $T_0(H)$ (or $H_0(T)$) is defined by $\mu_0 = 0$. Hereafter, $T_0(0)$ is often written merely as T_0. Detailed forms of γ_n and μ_n will be given separately in the following sections. On the other hand, no n-dependence of the coefficients b and b_p need to be specified throughout
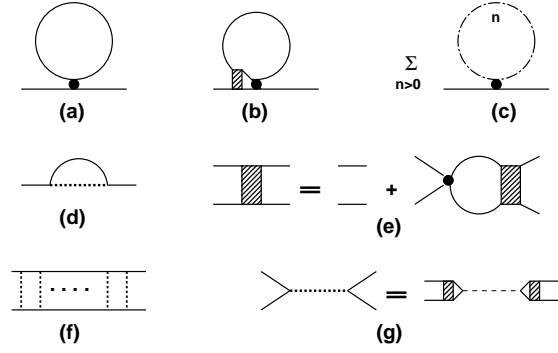
Fig. 2. Diagrams expressing the four terms of r.h.s. of eq.(4) ((a) to (d)) and the VG susceptibility (f). The interaction vertex correction (the hatched rectangle) is expressed in the diagram (e), and the diagram (g) defines $\tilde{b}_p$. The solid lines, the solid dots, the chain line, and the thin dashed line in (g) express, respectively, $\mathcal{G}_0$, b, $\mathcal{G}_n$ $(n \geq 1)$, and b_p.

this paper, since a high H approximation is invoked below in obtaining expressions useful for analyzing experimental data, and hence, the mutual interaction between the SC fluctuations and the interaction between a fluctuation and the random potential u are considered primarily within the lowest LL (LLL) with $n = 0$. In particular, in examining the data of cuprates and organics in which microscopic descriptions are still controversial, it is appropriate to assume that b is one of material parameters related to the magnetic penetration depth $\lambda(0)$, while the pinning strength b_p is an extrinsic parameter dependent on real samples used in experiments.

To renormalize the ψ-fluctuation with low energy, the LLL approximation will be used. That is, a relatively high field range is assumed, in which the renormalized energy scales (masses) of higher $(n \geq 1)$ LL fluctuations are much larger than that of LLL and do not deviate remarkably from their bare ones μ_n less sensitive to T compared with μ_0. Then, the renormalization of higher LL modes can be assumed to have already been accomplished independently. Further, the vortex pinning effect in the LLL-fluctuation renormalization will be incorporated to the one loop order.[23] Then, the *renormalized* LLL fluctuation propagator $\mathcal{G}_0(|\omega|)$ is determined by

$$(\mathcal{G}_0(|\omega|))^{-1} - \gamma_0|\omega| - \mu_0 = \Sigma_0 + \Delta\Sigma_l \tag{4}$$

$$+\Delta\Sigma_h - \frac{\tilde{b}_p}{2\pi r_B^2 d}\mathcal{G}_0(|\omega|).$$

Diagrams for the four terms of the r.h.s. of eq.(4) are given by Fig.2 (a) to (d). Here, the factor $\tilde{b}_p$ is a renormalized pinning vertex, sketched in Fig.2 (g), and is given by

$$\tilde{b}_p = b_p \int \frac{d^2 k}{2\pi} e^{-\mathbf{k}^2/2}(1 + u_v e^{-\mathbf{k}^2/2})^{-2} = \frac{b_p}{1 + u_v}, \tag{5}$$

where $u_v = b\beta^{-1}\sum_\omega \mathcal{G}_0^2(|\omega|)/(2\pi r_B^2 d)$. Consistently with this approximation, the VG transi-tioin point defined in the Gaussian approximation of VG fluctuation (i.e., the mean field VG

transition point) is determined according to the ladder diagram Fig.2 (f) expressing the VG susceptibility[23] as the limit $\mu_{\mathrm{vg},0} \to +0$, where

$$\mu_{\mathrm{vg},0} = 1 - \frac{\tilde{b}_p [\mathcal{G}_0(0)]^2}{2\pi r_B^2 d}. \tag{6}$$

Although, strictly speaking, this pinning-renormalization replacing b_p by $\tilde{b}_p$ is merely valid far above the vortex-solidification line in the pinning-free limit[4] and is diagrammatically consistent just with the pinning-free fluctuation renormalization in the case with no $\Delta\Sigma_l$ (see below regarding $\Delta\Sigma_l$), this approximation will be used hereafter for practical purposes because all resistivity data we will examine below belong to the cases where the first order vortex solid-liquid transition was destroyed by the pinning.

The main roles of LLL mass renormalization are played by the Hartree term Σ_0 of the self energy corresponding to Fig.2 (a) and expressed as

$$\Sigma_0 = \frac{b}{2\pi r_B^2 d\beta} \sum_\omega \mathcal{G}_0(|\omega|). \tag{7}$$

For the coefficient b, the ordinary GL expression[1] $16\pi^2 \lambda(0)^2/(\phi_0 H_0)$ in low H/H_0 will be used near and below $T_{c2}^*(H)$. The validity of this identification will be discussed in §6 in relation to the cuprates. Regarding the additional renormalization (correction) term $\Delta\Sigma_l$ within the LLL, an approximation of RPA type sketched in Fig.2 (b)

$$\Delta\Sigma_l = \beta^{-1} \sum_\omega \mathcal{G}_0(|\omega|) \frac{\ln[1 + bE_{00}(|\omega|)/(\pi r_B^2 d)]}{2E_{00}(|\omega|)}, \tag{8}$$

(see eq.(2.11) of ref.21) will be useful below, where $E_{00}(|\Omega|) = \beta^{-1} \sum_\omega \mathcal{G}_0(|\omega|)\mathcal{G}_0(|\omega+\Omega|)$. The term $\Delta\Sigma_l$ is negligible in the thermal 2D case[1] and, as far as a qualitative study of resistivity curves is concerned, may be negligible even in the quantum 2D case. However, to make sure, this term will be included when attempting to fit resistivity data in §3 and 4.

The term $\Delta\Sigma_h$ implies higher LL contributions to the LLL mass renormalization. It should be remarked[32] that the higher LL fluctuations are not negligible even in the present high H approximation but do contribute to a downward shift of $T_0(H)$ to $T_{c2}^*(H)$ corresponding to the apparent upper critical field $H_{c2}^*(T)$, just like in zero field case[33] where a reduction ΔT_c of the mean field transition point is ascribed to the amplitude-dominated fluctuation with *high* energy. This downward shift is conveniently represented, as in Fig.2 (c), by a sum of Hartree diagrams. The resulting temperature $T_0 - \Delta T_c$ corresponds not to the true SC transition point T_c at which the linear resistance vanishes but, roughly speaking, to an onset of a sharp resistive vanishing or of the critical region accompanying the transition at T_c. Rather than T_c, this resistive onset, denoted as T_{c0} hereafter, appears in the ensuing expressions for $H \neq 0$. Since Fig.2 (c) is ultraviolet divergent even in 2D case when the quantum fluctuation is included, its H-dependence is a correction, and hence, $\Delta\Sigma_h$ may be identified with its expression in $H = 0$ case. Further, when the presence of other non-SC order parameter fluctuations coupling
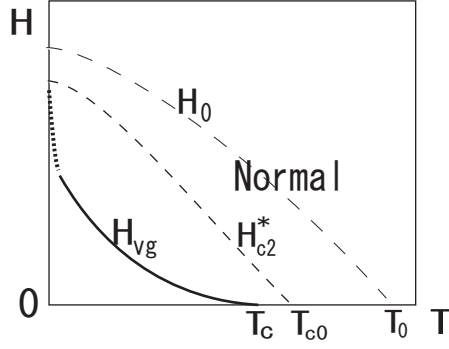
Fig. 3. Schematic H-T diagram in which various crossover or transition curves defined in the text are drawn. The low H limit of $H_{\rm vg}(T)$-line corresponds to T_c.

to the SC fluctuation is not negligible as in the underdoped cuprates (§3), they should also be incorporated into $\Delta\Sigma_h$. It will be argued in §3 that even such non-SC fluctuations do not bring additional H-dependences. Then, $\Delta\Sigma_h$ may be written as $\ln(T_0/T_{c0})$,[21, 32] and the $T_{c2}^*(H)$-line, reducing to T_{c0} in $H \to 0$ limit, is determined by $\mu_0 + \Delta\Sigma_h = 0$. In Fig.3, the characteristic temperatures and fields defined above are sketched in the H-T diagram.

Due to the presence of the pinning term $\propto \tilde{b}_p$, solving eq.(4) selfconsistently requires not a difficult but a very cumbersome numerical-integration even if neglecting $\Delta\Sigma_l$. A more cumbersome situation is encountered[23] when trying to present a practical expression on the VG contribution $\sigma_{\rm vg}$ to the conductivity. Since providing theoretical formulas useful in analyzing experimental data is the main purpose in this section, we will not try to give a selfconsistent solution of eq.(4) but invoke the following approximation to give practically convenient expressions: The form $\mathcal{G}_0(|\omega|) = (\,\gamma_0|\omega| + (\mathcal{G}_0(0))^{-1}\,)^{-1}$ will be assumed. That is, any pinning-induced renormalization of frequency dependences will be neglected. Then, eq.(4) is replaced by

$$(\mathcal{G}_0(0))^{-1} = \mu_0 + \ln(T_0/T_{c0}) + \Sigma_0 + \Delta\Sigma_l - \frac{\tilde{b}_p}{2\pi r_B^2 d}\mathcal{G}_0(0). \tag{9}$$

Consistently with this, Σ_0 is represented as

$$\Sigma_0 = \frac{b}{2\pi^2 r_B^2 d\gamma_0} \int_0^{\epsilon_c} d\epsilon \, \coth\left(\frac{\beta\epsilon}{2\gamma_0}\right) \frac{\epsilon}{\epsilon^2 + (\mathcal{G}_0(0))^{-2}}, \tag{10}$$

where the cutoff ϵ_c is a constant of order unity, and $E_{00}(\omega)$ becomes

$$E_{00}(|\Omega|) = \beta^{-1} \sum_\omega \mathcal{G}_0(|\omega| + |\Omega|)\,\mathcal{G}_0(|\omega|) \tag{11}$$

$$\times \left(1 + \frac{\gamma_0|\Omega|}{2}\mathcal{G}_0(|\Omega|/2)\right)$$

after simply arranging the ω-summation. Although, strictly speaking, this simplification is valid when $1 - \mu_{g,0} \ll 1$, its justification should be discussed rather through a fitting to experimental data. Through computations leading to the results in the ensuing sections, we verified that refining this approximation was unnecessary except in s-wave disordered films at low enough temperatures (see §5).

Next, bearing eq.(9) describing the SC fluctuation in LLL in mind, expressions of transport quantities will be derived in terms of Kubo formula for them. The superconducting part σ_s of the electric (diagonal) conductivity is written in the form

$$d\,\sigma_s = \left(-\frac{\partial}{\partial\Omega}\right)\left.\overline{\langle j_{e,\,x}(-\mathrm{i}\Omega)\,j_{e,\,x}(\mathrm{i}\Omega)\rangle}\right|_{\Omega\to+0}, \tag{12}$$

where the overbar (bracket $\langle\ \rangle$) implies the random (ψ) average. The corresponding expression of the transport entropy s_ϕ is naively assumed to take the form[34]

$$d\,s_\phi = \beta\phi_0\left(-\frac{\partial}{\partial\Omega}\right)\left.\overline{\langle j_{e,\,x}(-\mathrm{i}\Omega)\,j_{h,\,y}(\mathrm{i}\Omega)\rangle}\right|_{\Omega\to+0} \tag{13}$$

(see, however, the next paragraph). If using the real time representation, the spatially-averaged electric and heat currents for the ordinary phenomenological GL model are given by

$$
\begin{aligned}
j_{e,\,x} &= \xi_0^2\frac{2\pi}{\phi_0}\langle\psi^*Q_x\psi + \mathrm{c.\ c}\rangle_{\mathrm{sp}}. \\
j_{h,\,y} &= \xi_0^2\langle\mathrm{i}[\partial_t\psi^*(t)]Q_y\psi(t) + \mathrm{c.\ c}\rangle_{\mathrm{sp}},
\end{aligned}
\tag{14}
$$

respectively, where t is the real time, and the bracket $\langle\ \rangle_{\mathrm{sp}}$ denotes the spatial average. Within the high H approximation in which $\mathbf{j}_e$ consists of LLL and the next lowest LL, the prefactor $\xi_0^2(2\pi/\phi_0)$ of $\mathbf{j}_e$ in eq.(14) generally becomes $\pi r_B^2/(\phi_0\,\mathcal{G}_1(0))$ in the vortex liquid region *irrespective of the microscopic details*. This fact proved in ref.23 (see eq.(2.23) there) is a direct consequence of gauge-invariance.

In contrast, the prefactor of $\mathbf{j}_h$ may be, at least at low T/T_0, strongly affected by a microscopic mechanism independent of the fluctuation property, and the correct s_ϕ should vanish in $T/T_0 \to 0$ limit. This issue in the s-wave case can be seen in ref.35. Since a correct magnitude of the prefactor of s_ϕ is unimportant for the purpose in this paper, for convenience, eq.(13) is used hereafter to obtain the transport energy U_ϕ. However, some comments on this point will be necessary because, strictly speaking, a *direct* use itself of eq.(13) in obtaining a correct U_ϕ is not justified. Based on microscopic and thermodynamic results,[35] the factor of $j_{h,y}$ in eq.(14) has to be doubled near T_{c0}, and a contribution $-\phi_0 M$ from the magnetization

current has to be subtracted from *the resulting* Ts_ϕ, where M (< 0) is the SC magnetization. As is well known, however, M in high fields, where the LLL approximation is useful, is always given, except a prefactor, by the mean squared pair-field $< |\psi|^2 >= \Sigma_0/b$, while we will explain below that the same thing holds true for Ts_ϕ given by eq.(13). Consequently, as far as the transport energy $U_\phi = Ts_\phi$ in LLL is concerned, U_ϕ defined by eq.(13) with eq.(14) coincides with a microscopically valid one.

Derivation of the term in σ_s with no pinning-induced vertex correction, denoted hereafter as $\sigma_{\rm fl}$, is almost the same as that in the pinning-free case.[4, 21] As already mentioned, the higher LLs are assumed to be inert in the LLL mass-renormalization by invoking a situation in high H or deep in the vortex liquid regime. In fact, reflecting the equivalence between the next lowest LL mode and the compressional elastic mode of the vortex liquid,[32] $(\mathcal{G}_1(0))^{-1}$ has to reduce in the vortex liquid regime to $\mu_1 - \mu_0$ insensitive to T. Further, within the high H approximation, fluctuation vertex corrections accompanied by an interaction between the LLL and the next lowest LL modes can be neglected in the $\sigma_{\rm fl}$-expression. Then, our calculation of $\sigma_{\rm fl}$ is the same as the previous one,[21] and one finds

$$dR_Q\sigma_{\rm fl} = \frac{\gamma_0}{2(\mathcal{G}_1(0))^2\beta} \sum_\omega \left[\mathcal{G}_0(\omega)\mathcal{G}_1(\omega)[\mathcal{G}_0(\omega) + g\mathcal{G}_1(\omega)] - \frac{(\mathcal{G}_0(\omega))^2 + g^2(\mathcal{G}_1(\omega))^2}{(\mathcal{G}_1(0))^{-1} + g(\mathcal{G}_0(0))^{-1}} \right] \quad (15)$$

$$= (\mathcal{G}_1(0))^{-2} \int \frac{d\epsilon}{2\pi} \frac{\beta\gamma_0\gamma_1\epsilon^2}{2\sinh^2(\beta\epsilon/2)} \frac{1}{(\gamma_0^2\epsilon^2 + (\mathcal{G}_0(0))^{-2})(\gamma_1^2\epsilon^2 + (\mathcal{G}_1(0))^{-2})},$$

where $g = \gamma_1/\gamma_0$, $\mathcal{G}_1(\omega) = (\gamma_1|\omega| + (\mathcal{G}_1(0))^{-1})^{-1}$, and the prefactor $(\mathcal{G}_1(0))^{-2}$ arises from the above-mentioned $\mathbf{j}_e$-vertices. As mentioned in ref.20, however, the details of $\mathcal{G}_1(0)$ are not reflected in computed results of $\sigma_{\rm fl}$, in most of the T and H ranges we have examined, as a result of the relation $\gamma_1\mathcal{G}_0(0)/(\gamma_0\mathcal{G}_1(0)) \ll 1$. For this reason,

$$(\mathcal{G}_1(0))^{-1} = \mu_1 - \mu_0 \quad (16)$$

will be assumed hereafter both above and below $T_{c2}^*(H)$. Clearly, $\sigma_{\rm fl}$ of eq.(15) vanishes in $T \to 0$ limit. Note that the neglect based on the high H approximation of the fluctuation vertex corrections in $\sigma_{\rm fl}$ does *not* conflict with the inclusion of $\Delta\Sigma_l$ in the mass renormalization.

In the realistic case with a vortex pinning, an additional contribution $\sigma_{\rm vg}$ to σ_s created by a pinning-induced vertex correction becomes divergent on approaching a 3D VG transition point $T_{\rm vg}$[5, 36] from above. Near $T_{\rm vg}$, the contribution of quantum SC fluctuation to $\sigma_{\rm vg}$ is negligible, and a $\sigma_{\rm vg}$-expression in the thermal case

$$dR_Q\sigma_{\rm vg} = c_p \frac{\gamma_0 T_{c0}}{(t - t_{\rm vg})^s}, \quad (17)$$

where $t = T/T_{c0}$, will be used in comparing our theory with experimental data by choosing $t_{\rm vg} = T_{\rm vg}/T_{c0}$ and the prefactor c_p as being sample-dependent (i.e., pinning-dependent and, in the case of cuprates, doping-dependent) parameters. Although the prefactor c_p should depend

not only on b_p and b (i.e., the pinning and fluctuation strengths in $H = 0$) but on H,[36] for simplicity, it will be assumed to be H-independent in §3 and 4. The exponent s is known to depend on the dimensionality of pinning potentials dominant in the sample we focus on, and, strictly speaking, it is difficult to predict an appropriate value of s through each fitting far above T_{vg}. Throughout the fittings to be explained below, $s = 4.0$ was always assumed.

On the other hand, in situations where the system is 2D-like in spite of the presence of pinning effect, a true divergence of σ_{vg} may not occur, and hence the quantum fluctuation contribution to σ_{vg} is not negligible. As an approximate σ_{vg}-expression appropriate to this situation, the expression derived within the Gaussian approximation in ref.23

$$dR_Q\sigma_{\text{vg}} = (\pi\beta)^{-1}\left(\frac{b_p\mathcal{G}_0(0)}{2\pi r_B^2 d}\right)^2\sum_\omega\frac{\partial}{\partial|\omega|}\left[\ln(1 + c_c^{-2}\xi_{\text{vg},0}^2)\frac{\mathcal{G}_0(\omega)}{2}(\mathcal{G}_0(\omega) + \mathcal{G}_0(0))\right. \quad (18)$$

$$\left. - (\mathcal{G}_0(\omega))^2\ln\left(\frac{1 + c_c^{-2}\xi_{\text{vg},0}^2 + 2|\omega|\gamma_0\mathcal{G}_0(0)[\xi_{\text{vg},0}]^4}{1 + 2|\omega|\gamma_0\mathcal{G}_0(0)[\xi_{\text{vg},0}]^4}\right)\right]$$

will be used below, where $\xi_{\text{vg},0} = \mu_{\text{vg}}^{-1/2}$ is the dimensionless VG correlation length expressed in unit of r_B, and $\mu_{\text{vg}} = \mu_{\text{vg},0} + \sqrt{\gamma_0 T\mathcal{G}_0(0)}$. This form of μ_{vg} is an expression useful for interpolation near an apparent 2D quantum VG transition field B_{vg}^*,[23] and the term $\sqrt{\gamma_0 T\mathcal{G}_0(0)}$ plays a role of modelling the presence of the quantum VG critical regime within the Gaussian approximation. Further, the constant c_c of order unity is related to an upper cutoff of the wavevector integrals and will be hereafter chosen as $c_c = 1$.

In general, σ_{vg} also vanishes in $T \to 0$ limit in $B > B_{\text{vg}}^*$, where B_{vg}^* is defined by $\mu_{\text{vg},0}(B = B_{\text{vg}}^*, T \to 0) \to 0$. Further, $\xi_{\text{vg},0}(B = B_{\text{vg}}^*, T) \propto T^{-1/4}$, and $dR_Q\sigma_{\text{vg}}(B = B_{\text{vg}}^*)$ is approximated by a *nonuniversal*[23,37] constant at low enough T where $\xi_{\text{vg},0} \gg 1$. Note that eq.(18) is an expression valid within the Gaussian approximation and hence, may diverge in $B < B_{\text{vg}}^*$ at a finite temperature like in 3D case. As is seen later in Fig.12, however, it is possible that it remains nondivergent at nonzero T, depending on the microscopic details. In the fittings, we will use either eqs.(16) or (18), depending upon the situations.

One might wonder if the fact that both of eqs.(15) and (18) in $B > B_{\text{vg}}^*$ vanish in low T limit is not a result of the neglect of some vertex corrections in the Kubo formulas. However, it was proved[21] at least in the pinning-free case that all terms including the vertex corrections vanish in low T limit. It is trivially performed to extend the proof in ref.21 to the case with vortex-pinning as follows. First, as in the electron systems,[38] as far as the conductivity *prior to* the random average is considered, the *fluctuation* propagators $\mathcal{G}_n(|\omega|)$ ($n \geq 0$) depend on two coordinates and can be represented in a form like $\mathcal{G}_n(|\omega|; \mathbf{r}_1, \mathbf{r}_2) = \sum_\mu u_\mu(\mathbf{r}_1)\mathcal{G}_{n,\mu}(|\omega|)u_\mu^*(\mathbf{r}_2)$ where u_μ is an eigen function specified by a quantum number μ. Since the proof in ref.21 is applied in the same way as far as the spectral form (i.e., frequency dependence) in the low frequency limit remains dissipative and is valid irrespective of the forms of coordinate or wavevector dependences of $\mathcal{G}_n$, it is concluded that the sum $\sigma_{\text{fl}} + \sigma_{\text{vg}}$ vanishes in low T limit

even if the vertex corrections are included. Therefore, by combining the high H approximation with this, the neglect of the vertex correction in eqs.(15) and (18) is safely valid.

Just as for the conductivity, the transport energy U_ϕ may also be examined by neglecting the vertex corrections in the Kubo formula because the heat current is also accompanied by the next lowest LL mode. On the other hand, the pinning-induced vertex correction related to the VG fluctuation may be neglected in s_ϕ assuming a weak pinning because no divergent contribution near T_{vg} will arise in this quantity as a result of the additional time-derivative in the $\mathbf{j}_h$-expression compared to the $\mathbf{j}_e$-one. By arranging the frequency summation to take the Ω-derivative, we obtain

$$
\begin{aligned}
s_\phi \;=\; & \frac{H}{dH_0(0)\mathcal{G}_1(0)} \sum_\omega \Bigg[\gamma_0\gamma_1 |\omega| ([\gamma_1\mathcal{G}_1(0)]^{-1} - [\gamma_0\mathcal{G}_0(0)]^{-1})(\mathcal{G}_0(\omega)\,\mathcal{G}_1(\omega))^2 \quad (19) \\[2mm]
+ \;& \frac{1}{(\gamma_0\mathcal{G}_0(0))^{-1} + (\gamma_1\mathcal{G}_1(0))^{-1}} \Bigg[([\gamma_1\mathcal{G}_1(0)]^{-1} - [\gamma_0\mathcal{G}_0(0)]^{-1})\mathcal{G}_0(\omega)\mathcal{G}_1(\omega) \\[2mm]
- \;& \frac{\gamma_0}{\gamma_1}|\omega|(\mathcal{G}_0(\omega))^2 + \frac{\gamma_1}{\gamma_0}|\omega|(\mathcal{G}_1(\omega))^2 \Bigg]\Bigg].
\end{aligned}
$$

In the present high H approximation, eq.(19) is simplified, by neglecting terms of higher order in $\gamma_1\mathcal{G}_1(0)/(\gamma_0\mathcal{G}_0(0))$, as

$$
U_\phi \simeq \frac{\beta^{-1}H}{H_0 d\mathcal{G}_1(0)} \sum_\omega \mathcal{G}_1(\omega)\mathcal{G}_0(\omega) \simeq \frac{\phi_0^2}{16\pi^2\lambda^2(0)}\Sigma_0, \tag{20}
$$

where, as mentioned earlier, the prefactor $(\mathcal{G}_1(0))^{-1}$ is carried by the $\mathbf{j}_e$-vertex. Namely, in the present high H approximation, s_ϕ in the GL region is proportional to the fluctuation entropy (i.e., the mean-squared pair-field) even in the quantum case, and the mean field result $\phi_0^2\beta(1 - T/T_{c0})/(16\pi^2\lambda^2(0))$ is expected to be recovered deep in the vortex liquid regime if the fluctuation has calmed down there.

In the following sections, the above expressions of σ_{fl}, σ_{vg}, and U_ϕ are used together with eqs.(5), (8), (9), (10), (11), and (16) to examine experimental data of transport quantities, primarily, of the resistivity

$$
\rho = (\sigma_n + \sigma_{\mathrm{fl}} + \sigma_{\mathrm{vg}})^{-1}, \tag{21}
$$

where the normal conductivity $\sigma_n(T)$ should be estimated through experimental $\rho(T)$ data in $T > T_{c0}$ by, as usual, neglecting its H-dependence and is implicitly assumed to include other fluctuation conductivity terms excluded from the GL description. The Nernst coefficient N, measured in refs.16 and 17, is defined as

$$
N = \frac{s_\phi\rho}{\phi_0}. \tag{22}
$$

We note that, since U_ϕ is proportional to $-\phi_0 M$ in the GL region, the magnetization M may be

chosen in place of U_ϕ as a quantity to be compared with ρ. Even if taking account of electronic details of materials of interest, $\lambda(0)$, T_0, H_0, and T_{c0} are independent SC material parameters in an ordinary microscopic description of superconductors. They appear in the coefficients of the GL action such as μ_0 and γ_0. On the other hand, $\sigma_n(T)$ is highly sensitive to the sample purity and can be seen as being independent of the four SC parameters mentioned above. In order to mimic a vanishing behavior of $\rho(T)$ far below T_{c0}, a VG term σ_{vg}, i.e., a (sample-dependent) vortex pinning effect on the conductivity, needs to be incorporated. If the 3D form, eq. (17), is used, its prefactor c_p and a form of transition line $t_{\mathrm{vg}}(H) = T_{\mathrm{vg}}(H)/T_{c0}$ are chosen to optimize the fittings. In general, the vortex pinning in real systems may occur due to crystal defects other than a microscopic impurity affecting σ_n, and further, the transition line $t_{\mathrm{vg}}(H)$ may not be described precisely in the LLL approximation assumed so far, once recalling a strong H-dependence of the vortex elastic moduli and the presence in real samples of a small amount of other pinning sites. That is, the vortex pinning should be regarded as being independent of σ_n and is not necessarily described in terms of a single extrinsic parameter. If the 2D form (18) is a more appropriate σ_{vg}, the pinning strength b_p is the only extrinsic (sample-specific) parameter at *nonzero* temperatures.

3. Cuprate Superconductors

In this section, the theoretical expressions in §2 will be applied to experimental data of superconducting cuprates. Since one purpose of examining resistivity data of cuprates is to correctly understand the doping dependences of fluctuation effects and of material parameters of cuprates, we will primarily examine resistivity data of LSCO of which an extensive doping dependence can be seen in the literature.[8] As shown in ref.20 where the expressions obtained in §2 were applied, data of other quantity measured consistently are also needed, together with resistivity data, to correctly estimate material parameters in cuprates with small condensation energy. In underdoped cuprates, such a set of data measured consistently are not known except the LSCO data in refs.16, 17, and 39. Below, we will proceed further the analysis to the overdope side and comment on other cuprate materials on the basis of available data.[26, 39]

Let us start with incorporating microscopic ingredients into the GL description. Since experimental data in several teslas are primarily examined for materials with a much lower $H_{c2}^*(0)$ than the optimally-doped YBCO, we need a reasonable functional form of $H_{c2}^*(T)$ which may not be approximated in several teslas as the ordinary linear straight line. Further, the time scales γ_n need to be calculated consistently with this $H_{c2}^*(T)$. To this end, we invoke the ordinary clean limit[40] in order to describe μ_n and γ_n consistently (see §2 on their definition). For simplicity, let us assume, as in the weak-coupling s-wave pairing case, a circular Fermi surface. Then, they are given by

$$\gamma_n = \frac{\beta}{2\pi} \int_0^\infty ds \frac{s}{\sinh(s)} \mathrm{L}_n(u_c^2 s^2) e^{-(u_c s)^2/2} , \tag{23}$$

$$\mu_n = \ln\left(\frac{T}{T_0}\right) + \int_0^\infty ds \, \frac{1 - \mathrm{L}_n(u_c^2 s^2) \, e^{-(u_c s)^2/2}}{\sinh(s)},$$

respectively, where $u_c = T_0\sqrt{H/(2H_0 e^\gamma)}/T$, $\mathrm{L}_n(x)$ is the n-th order Laguerre polynomial, and $\gamma = 0.5771$ is the Euler constant which should not be confused with the time scales γ_n.[41,42] It is valuable to comment on the fact that γ_n with any odd integer n approaches zero in $T \to 0$. Since an equilibrium vortex solid state with no Pauli limiting effect is represented by the LLs with even n, a dissipative vortex flow motion is created by other odd LLs[32] so that the vortex flow conductivity is proportional to γ_n with an odd n. Hence, this result suggestive of dissipation-free vortex flow at $T = 0$ in clean limit may be rather expected and significantly enhances the quantum *resistive* behaviors in cuprates and organics at *finite* temperatures.

As noted in §2, the apparent upper critical field line $H_{c2}^*(T)$ approaching T_{c0} in low H limit (see Fig.3) is determined by $\mu_0 + \Delta\Sigma_h = 0$. When $\Delta\Sigma_h = \ln(T_0/T_{c0})$, we obtain

$$H_{c2}^*(T) = H_0\left(\frac{T_{c0}}{T_0}\right)^2 \Phi(t), \tag{24}$$

from eq.(23), while $H_0(T)$ is given by $H_0\Phi(T/T_0)$, where the function $\Phi(x)$ satisfies $\Phi(0) = 1$ and $\Phi(1) = 0$. In particular, a large enough value of the parameter T_0/T_{c0} significantly affects fluctuation phenomena in nonzero fields.

Note that, when T_{c0} rather than T_0 is chosen as a temperature parameter scaling T, H_0 is replaced by $H_{c2}^*(0) = H_0(T_{c0}/T_0)^2$. By combining this with eqs.(4) and (11), we find the property

$$\sigma_{\mathrm{fl}}(T_0/T_{c0}, H_0, \lambda(0)) = \sigma_{\mathrm{fl}}(1, H_{c2}^*(0), T_{c0}\lambda(0)/T_0) \tag{25}$$

to be valid in the high H approximation. Namely, if the SC pseudogap region with the width $T_0 - T_{c0}$ is neglected, $\xi_0 = \sqrt{\phi_0/(2\pi H_0)}$ is overestimated, while $\lambda(0)$ is underestimated. A discussion based on this fact will be given in §6.

As the first example of comparisons with data, the case of optimally-doped YBCO shown in Fig.1 (a) will be explained. In this case, the $\rho(T)$ curves in the tesla range show the fan-shaped broadening in the thermally-induced vortex liquid region below T_{c0}, and the thermal SC fluctuation reduces ρ-values near $T_{c2}^*(H)$ compared with the mean field result of resistivity. Figure 1(a) includes 12 (T) data in ref.22 and $\rho(T)$ curves computed in terms of the material parameters given in Table I, while the curves in Fig.1 (b) result from the same set of material parameters, except $\lambda(0) = 0.35$ (μm), as in Fig.1 (a). Further, the normal resistivity $\sigma_n^{-1} = 0.135T/T_{c0}(\mathrm{m}\Omega.\mathrm{cm})$ and the 3D-like σ_{vg}, eq.(17), with $c_p = 1.3 \times 10^{-4}$ and $t_{\mathrm{vg}} = 1 - h - 1.2h^{2/3}$, where $h = H/H_{c2}^*(0) \ll 1$, were assumed. Since, in several teslas, the h-values of optimally-doped YBCO are much lower than those in most of underdoped and overdoped materials including LSCOs to be discussed below, an additional contribution[1] composed only of *thermal* higher LL modes to σ_f was also included in obtaining the solid curves together with the quantum contribution accommodated in eq.(15). In Fig.1 (a), however, a change of
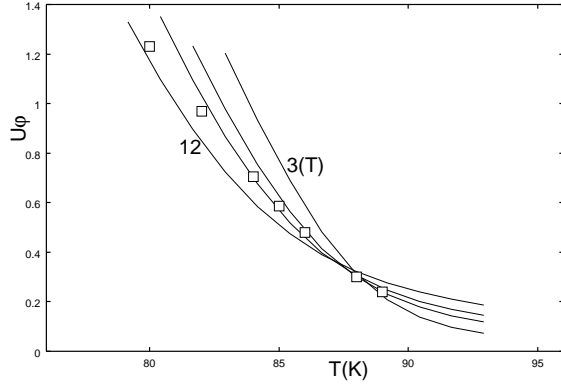
Fig. 4. U_ϕ-curves (solid curves) at 3, 6, 8, and 12 (T) obtained consistently with those in Fig.1 (a) and 12 (T) data (open squares).[22] In this and other figures of $U_\phi(T)$, U_ϕ is represented in unit of 10^{-12}(J/m).

resistivity value brought by the addition of higher LL contributions is within several percents in magnitude, and the quantum contribution was quite negligible. The positions of $H_{c2}^*(T)$ for each resistivity curve are denoted by filled circles both in Fig.1 (b) and the figures appearing hereafter. Further, we note that, although a small but nonvanishing $T_0/T_{c0} - 1$ was taken into account in Fig.1 favoring an agreement with the consistent data of U_ϕ (see Fig.4), the obtained values of $\lambda(0)$ and ξ_0 remained unchanged compared with those in previous fittings[1] where the quantum contribution was neglected from the outset.

We note that T_0 we define is the bare mean field SC transition point defined *prior to* including a coupling with possible non SC orderings competing with the SC ordering. We expect two types of origins of the SC pseudogap region $T_0 - T_{c0}$ in cuprates. First, inclusion of a fluctuation of a competing non-SC ordering, such as a spin or charge ordering, coupling to the SC order parameter can lead to a reduction of the mean field (MF) SC transition point. The resulting MF transition temperature in $H = 0$ will be called T_c^{MF} hereafter. This can be modelled by adding the term

$$\mathcal{S}_x = u_x \int_\tau \int d^2r |\phi_{ns}|^2 |\psi|^2 \tag{26}$$

in GL action, where ϕ_{ns} denotes a non-SC order parameter fluctuation, and only a fluctuation competitive (or repulsive) to ψ is assumed here through the condition $u_x > 0$. Since $|\phi_{ns}|^2$ is replaced by the averaged value $< |\phi_{ns}|^2 >$ in constructing an effective action on ψ, T_c^{MF} will be expressed as $T_0 \exp(-u_x < |\phi_{ns}|^2 >) \ (< T_0)$, and consequently, we has only to replace $\ln(T/T_0)$ in μ_0 by $\ln(T/T_c^{\mathrm{MF}})$, where $< |\phi_{ns}|^2 >$ was assumed to be H-independent. The second origin of T_0-shift is nothing but $\Delta\Sigma_h$ in the LLL mass renormalization outlined in §2, where it was assumed to arise entirely from the SC fluctuation in higher LLs. An additional contribution to $\Delta\Sigma_h$ also arises from $\mathcal{S}_x$ and similar higher order coupling terms between ψ-fluctuations and ϕ_{ns}. As in §2, by assuming this contribution to $\Delta\Sigma_h$ of such a ϕ_{ns}-fluctuation

	Fig.1(a), 4	Fig.5	Fig.8
$\lambda(0)$ (μm)	0.11	0.43	1.9
H_0 (T)	272	235	330
T_0 (K)	120	96	90
T_{c0} (K)	92	32	15
d (nm)	1.5	1.5	1.5

Table I.   Material parameter values used in Figs.1, 4, 5, and 8. Parameters related to the pinning effect and σ_n are given in the text.
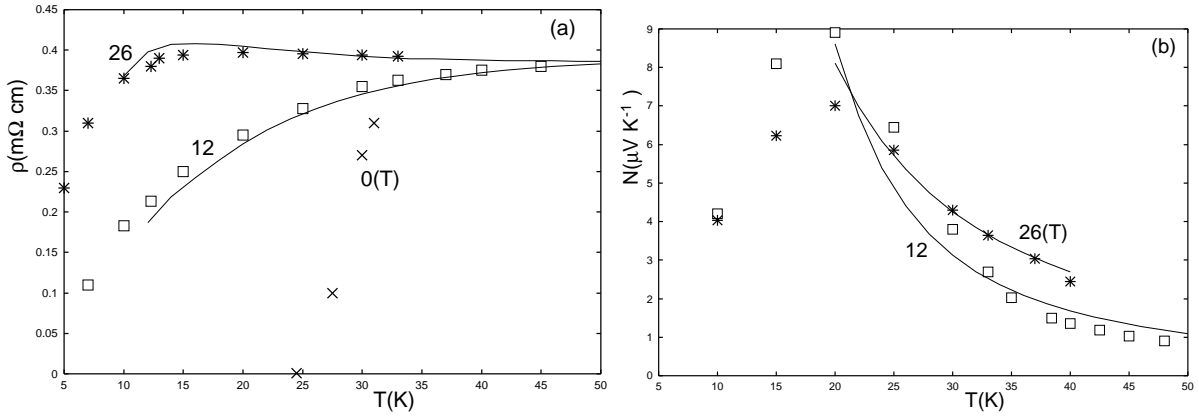

Fig. 5.   Fittings to LSCO $x = 0.08$ data at 12 and 26 (T) of (a) ρ and (b) N in Ref.16.

to be also H-independent, $\Delta\Sigma_h$ can be identified with $\ln(T_c^{\mathrm{MF}}/T_{c0})$. That is, T_c^{MF} does not appear in $\mu_0 + \Delta\Sigma_h$.

The assumption of H-independence of the ϕ_{ns}-fluctuation can be justified by comparing with experimental observations as follows. First, according to NMR measurements[43] in the pseudogap regime, the antiferromagnetic (AF) fluctuation, which is competitive with the SC fluctuation and should be dominant in the NMR signal in the nodal directions, is suggested to be insensitive to H at least in $T > T_{c0}$. On the other hand, a local AF ordering was shown to be enhanced with increasing H primarily below the irreversibility line where the ohmic resistivity is absent.[44] This H-dependence of AF ordering is essentially linear in H, reflecting the number of vortices, and possibly, will be a consequence of the spatial variation of $|\psi|$ near the vortex cores.[45, 46] However, in the high H approach of GL theory, the spatial variation of $|\psi|$ is reflected only in $\beta_A - 1$ which is negligible[4] in discussing thermodynamics and transport phenomena above the irreversibility line (i.e., in the vortex liquid regime). Therefore, we believe that the assumption of H-independence of ϕ_{ns}-fluctuation is valid in the vortex liquid regime. Even if the ϕ_{ns}-fluctuation induces an H-dependence in the effective action on the ψ-fluctuation, both fluctuations are competitive with each other, and hence, a SC
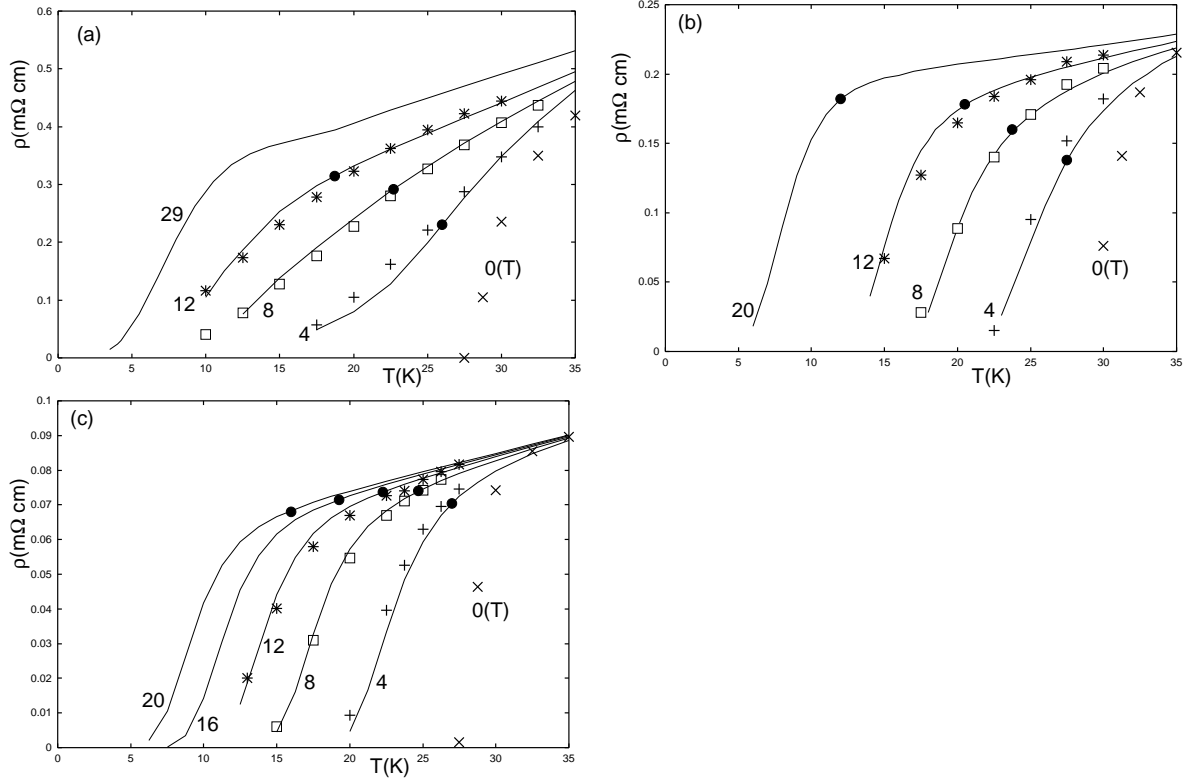
Fig. 6. Resistivity data (symbols)[8] of LSCO in the same temperature range at three doping levels (a) $x = 0.08$, (b) 0.15, and (c) 0.2 and corresponding theoretical results (solid curves). The darked circle on each $\rho(T)$ curve denotes $T_{c2}^*(H)$ in each H.

coherence length defined from a H-dependence in the effective action would be enhanced by the presence of ϕ_{ns}-fluctuations. As is repeatedly seen hereafter, however, ξ_0-values resulting from the fittings to data of underdoped cuprates already become short enough. For this reason, the extra H-dependence due to the ϕ_{ns}-fluctuations is likely to be quantitatively negligible, and hence, we assume the contributions of ϕ_{ns}-fluctuation to have been fully accommodated as $\ln(T_0/T_c^{\mathrm{MF}})$. Although, as a result of this, T_c^{MF} does *not* appear in the r.h.s. of eqs.(4) and (9), the mean field transition field in the presence of ϕ_{ns}-fluctuations will be given, consistently with eq.(24), by $H_0(T_c^{\mathrm{MF}}/T_0)^2\Phi(T/T_c^{\mathrm{MF}})$ which may decrease with underdoping. Note, nevertheless, that the genuine ξ_0 is defined through the microscopic field scale H_0 *irrespective of ϕ_{ns}-fluctuations.*

Based on the inclusion, explained above, of competing ϕ_{ns}-fluctuations, the fitting results to LSCOx data with $x = 0.06$ and 0.08 reported in ref.20 will be commented on here. Hereafter, in considering the doping dependence of cuprates, the spacing d between the SC layers will be fixed. In ref.20, the formulas given in §2 were applied by neglecting the difference between T_0 and T_c^{MF}. Regarding σ_{vg}, eq.(17) with $c_p = 10^{-2}$ was used for $x = 0.08$ case, and eq.(18) with $b_p = (2\pi\xi_0^2 d)0.023$ was applied to $x = 0.06$ case . According to the results in ref.20,
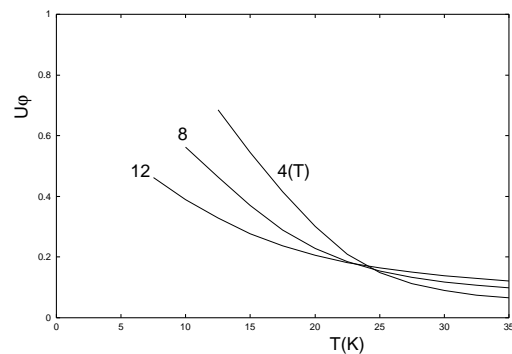
Fig. 7. U_ϕ-curves corresponding to ρ-curves in Fig.6 (c).

$T_0(x)$ became insensitive to x in $x < 0.1$ in contrast to T_ν, defined in ref.26 as the onset of SC Nernst signal, which *decreases* with decreasing x (< 0.1). Here, in relation to Fig.6 (a) below, the fitting results to the $x = 0.08$ data given as Fig.2 in ref.20 will be shown again in Fig.5, where $(\sigma_n)^{-1} = 0.02905 \ln(1.6 \times 10^6 T_{c0}/T)$ (mΩ.cm) and the parameters listed in Table I were used. Regarding the $x = 0.06$ case, it has been noticed recently that, even if assuming T_0 to increase with decreasing x just like T_ν in Bi-compounds,[26] the data can be quantitatively explained. For instance, the parameter values $\lambda(0) = 2.3(\mu\text{m})$, $T_0 = 100(\text{K})$, $T_{c0} = 13(\text{K})$, $H_0 = 493(\text{T})$, and $(\sigma_n)^{-1} = 0.0994 \ln(186.3 T_{c0}/T)$ (mΩ.cm) were used for the $x = 0.06$ case, and the obtained curves of ρ and N were almost the same as those in Fig.1 of ref.20 where a smaller T_0 value, 96(K), was assumed. Contrary to this, no choice of T_0 decreasing with underdoping has resulted in a consistency with the Nernst data[16] particularly in the $x = 0.06$ case. What corresponds to T_ν in low H limit is the mean field transition point T_c^{MF}. More accurately, because the Nernst signal due to *Gaussian* SC fluctuation is usually nonzero above the microscopic transition point, T_c^{MF} may lie slightly below T_ν. Hence, T_ν in $x < 0.1$ of LSCO, showing the unexpected doping dependence, will correspond to T_c^{MF} affected by competing non-SC fluctuations becoming stronger with underdoping. That is, we expect T_0 in LSCO to, contrary to T_c^{MF}, increase with underdoping like in the Bi-compounds.[26]

Next, in relation to Fig.5, the doping dependence of resistivity curves will be examined in order to corroborate that doping dependences of material parameters predicted in ref.20 are valid over a wider doping range including the overdoped side. Previously, a systematic study of resistive behaviors at various doping levels of LSCO was reported,[8] and the data in ref.8 will be used here. We focus on the temperature range $10 < T(\text{K}) < 35$ and approximate each $[\sigma_n(T)]^{-1}$ curve there via a T-linear curve. Among various data in ref.8, we have examined three doping levels, $x = 0.08$ (underdoped case), $x = 0.15$ (nearly optimal case), and $x = 0.2$ (slightly overdoped case). Fluctuation effects in strongly overdoped materials ($x \geq 0.24$) are expected to be quite weak, and those data will not be considered here. First of all, the $x = 0.08$ data have been fitted by assuming a T_0/T_{c0} value similar to that in Fig.5. Next, the

x	0.08	0.15	0.2
$\lambda(0)$ (μm)	0.57	0.46	0.417
H_0 (T)	245	190	55.1
T_0 (K)	100	86.5	40.5
T_{c0} (K)	30	31	30
d (nm)	1.5	1.5	1.5
σ_n^{-1} (mΩ cm)	$0.245 + 0.27t$	$0.19 + 0.0426t$	$0.055 + 0.0312t$
c_p	0.04	0.01	0.033
$\alpha_{\rm vg}$	0.5	0.67	0.67
$\beta_{\rm vg}$	3.4	0.8	2.26
$H_c(0)$ (T)	0.352	0.385	0.23

Table II.   Parameter values used in computation of resistivity curves in each figure of Fig.6. The
parameter t denotes T/T_{c0}.

parameter values for $x = 0.2$ case were chosen by favoring a semiquantitative agreement with
Nernst data in ref.17 (see Fig.1 there). Then, in $x = 0.15$ case, a T_0/T_{c0} value intermediate
between the 0.08 and 0.2 cases was assumed. However, according to eq.(25), the key parameter
in comparing with ρ data is the product $\lambda(0)\xi_0$, that is, $H_c(0) = (\lambda(0))^{-1}\sqrt{\phi_0 H_0/4\pi}$ (see
eq.(2)) which is independent of T_0 in GL theory. The obtained curves are shown together
with the data[8] in Fig.6, and the values of material parameters used for fittings are listed
in Table.II. The parameters $\alpha_{\rm vg}$ and $\beta_{\rm vg}$ are included in the assumed form of VG transition
curve $t_{\rm vg}(h) = T_{\rm vg}(h)/T_{c0} = (1 - h)/(1 + \beta_{\rm vg}h^{\alpha_{\rm vg}})$, where $h = H/H_{c2}^*(0)$. This expression of
$t_{\rm vg}(h)$ is based upon the VG transition line in the mean field approximation derived within
the LLL.[4] The factor $1 - h$ arises from the mean-squared amplitude of the pair-field, while the
exponent $\alpha_{\rm vg}$ depends upon the dimensionality of SC fluctuation and takes 0.5 and 0.67 in its
2D and 3D limits, respectively. This $\alpha_{\rm vg}$ is a direct measure of the sample anisotropy in the
present approach applicable primarily to 2D-like materials (see the second paragraph of §2).
The $\alpha_{\rm vg}$ values shown in Table II are compatible with the well-known fact that the hole-doped
cuprate materials are more 2D-like with underdoping. By contrast, $\beta_{\rm vg}$ is sample-specific and
also depends on both of the fluctuation strength and the pinning strength. Furthermore, there
are at least two ingredients affecting the form of $t_{\rm vg}(H)$ in realistic cases. One is an ingredient
independent of pinning effects and induces a deviation of $t_{\rm vg}$-form from its LLL expression.
Physically, a detail of the vortex elasticity, such as the H-dependence of the shear modulus of
a vortex lattice defined locally, will affect the form of $t_{\rm vg}(H)$, and hence, it is not surprising
that such a difference of the local shear modulus in $h < 1$ from its LLL expression affects the
$t_{\rm vg}(H)$-expression. Secondly, a small amount of line-like (or plane-like) pinning disorders in real
systems also affect the transition line. For instance, in real systems including both point-like

and line-like pinning disorders, the functional form of $t_{vg}(h)$ depends even on the h-values.[4] Thus, in fitting to resistivity data, it may be rather necessary to include a possible deviation of the $t_{vg}(H)$-form from the expression in LLL and in the purely point disorder case. To reduce the fitting parameters as far as possible, we have assumed that such involved ingredients will be incorporated by taking β_{vg} as a sample-specific fitting parameter independent of other material parameters. Nevertheless, it should be stressed that the details of the extrinsic parameters c_p and $t_{vg}(h)$ should not be important for our purpose in this section of clarifying the doping dependence of *intrinsic* material parameters which are determined, roughly speaking, through the (pinning-independent) upper-half of the resistivity curves.

In lower fields in $x = 0.08$, the resistivity curves have the fan-shaped broadening suggestive of a dominance of thermal fluctuation over the quantum contribution. One might wonder if the result in Fig.6 (a) that the thermal (fan-shaped) behavior in lower fields is more evident with underdoping is consistent with the result[20] on *strongly* underdoped ($x < 0.1$) cases[11,16] where the thermal behavior was lost with underdoping in $x < 0.1$. This apparently conflicting result is resolved as follows. In the case of underdoped cuprates in tesla range, a strong SC fluctuation near T_0 is weakened to some extent upon cooling down to T_{c0} and behaves, much below T_0, like that in effectively higher fields. Roughly speaking, such a reduction of fluctuation arises from an increase, upon cooling in $T_{c0} < T < T_0$, of the coefficient of the gradient term in the $H = 0$ GL-expression. That is, the enhanced quantum fluctuation due to $\lambda(0)$ increasing with underdoping is partly compensated by the existence of a large SC pseudogap region which, in turn, results in weakening the fluctuation near and below T_{c0}. Hence, due to a T-dependence of an electronic origin, a long $\lambda(0)$ may not necessarily result in a quantum fluctuation-dominated behavior near T_{c0} in the tesla range. Actually, in contrast to LSCO in $x > 0.1$, the quantum fluctuation effect on $\rho(T)$ seems to be *monotonously* enhanced with underdoping in any H in the case of YBCO.[11,47]

In Fig.6 (a), no $H_{c2}^*(T)$ position (dark circle) on the 29(T) curve was indicated. Actually, $H_{c2}^*(0)$ for Fig.6 (a) is close to 21(T), and hence, this 29 (T) curve is an example of the case in which the pinning-induced drop of resistivity occurs above $H_{c2}^*(T)$ as a consequence of a broad SC pseudogap region. It is not surprising because a VG transition can occur anywhere in $T < T_0(H)$, i.e., as far as the SC fluctuation is present. A similar feature will be discussed again in §6.

In contrast, the resistivity curves in $x = 0.2$ and 0.15 cases always show a sharp drop. As suggested in ref.17, the high field ρ curves in $x = 0.2$ case show a sharp drop far below $H_{c2}^*(T)$ (dark circle) suggested from Nernst data, and hence the situation is likely to be similar to Fig.1 (b) in Introduction. Actually, the much weaker H-dependence of ρ around T_{c0} in $x = 0.2$ compared with that in $x = 0.15$ case is apparently inconsistent with an expected growth of ξ_0 accomanying the overdoping and rather reflects a fluctuation enhanced with

overdoping. This is due to $\lambda(0)\xi_0$ increasing with overdoping starting from the optimal-doping, although the $H = 0$ fluctuation is weakened with overdoping (see §1). The U_ϕ-curves computed consistently with Fig.6 (c) are shown in Fig.7. The obtained U_ϕ values and H-dependences semiquantitatively agree with the data shown in Fig.1 of ref.17. Properties of the U_ϕ curves are typically thermal, and, at least below 12 (T), there are no remarkable quantum fluctuation effect on U_ϕ. Regarding the $x = 0.15$ case, we note that the VG transition position $t_{\mathrm{vg}}(h)$ is closer to $H_{c2}^*(T)$-line compared with those in $x = 0.08$ and 0.2 cases, and that, due to this, the sharp ρ-drop in $x = 0.15$ case is rather similar to that in the mean field-like case with negligible vortex liquid region. This narrow vortex liquid regime suggested by the $x = 0.15$ data may be realized if the effective pinning strength *relative to* the fluctuation strength is maximal near the optimal doping.

One of important consequences arising from the fittings is that $[H_c(0)]^{-1} \propto \lambda(0)\xi_0$, i.e, the fluctuation strength in fixed H-values (see eq.(2)), is mimimal near the optimal doping and, just like $(T_{c0})^{-1}$, increases with *both* underdoping and overdoping from the optimal case. This is qualitatively consistent with the doping dependence of condensation energy density $[H_c(0)]^2/(4\pi)$ estimated from the heat capacity data.[48] It is easily understood by recalling the discussion on eq.(2) in §1 that the doping dependence of $\rho(T)$ curves mentioned in §1, including the fact that the fan-shaped resistive broadening is typically seen only near the optimal doping, is a reflection of this doping dependence of $H_c(0)$. Further, as Table II shows, the in-plane coherence length ξ_0 to be defined from H_0 monotonously decreases with underdoping over all doping ranges including $x < 0.1$.[20] This conclusion cannot be reached once the presence of the SC pseudogap region widening with underdoping is neglected.[47]

Examples of ρ and U_ϕ curves in a case with very large strengths of *both* the SC fluctuation and pinning effect are shown in Fig.8. They have been computed by bearing very underdoped Bi-2201 data[39] in mind (see Fig.2 in ref.39). A quantitative comparison with the data will not be attempted here because the data were taken on a film sample with a broadening of $\rho(H = 0)$ curve over 10 (K). This sample-specific broadening at $H = 0$ should be also reflected in low H curves of resistivity and make comparison of computed curves with the low H data difficult. Nevertheless, we expect semiquantitative features of the Bi-2201 data except ρ-curves below 6(T) to be comparable with Fig.8. As well as in the LSCO case with $x = 0.06$,[20] the 2D σ_{vg} expression, eq.(18), was used with $b_p = (2\pi\xi_0^2 d)0.15$. In Fig.8, $(\sigma_n)^{-1} = 0.21\ln(280\,T_{c0}/T))$ (mΩ.cm) was used together with the parameters shown in Table I. Qualitatively, the features are also similar to the LSCO data in $x \leq 0.06$.[14, 20] First, the quantum SC fluctuation in Fig.8 is strong. In fact, T_{c2}^* at 8(T) is close to 5(K) where the $\rho(T)$-curve is insulating. More notably, the resistivity curves above 5(K) suggest a 2D FSIT with $B_c^* \simeq 6$(T), like in Fig.1 of ref.20. However, the FSIT behavior in Fig.8 is more remarkable compared to the LSCO case with $x = 0.06$.[20] This is a consequence of the larger value of pinning strength b_p. Namely, a large
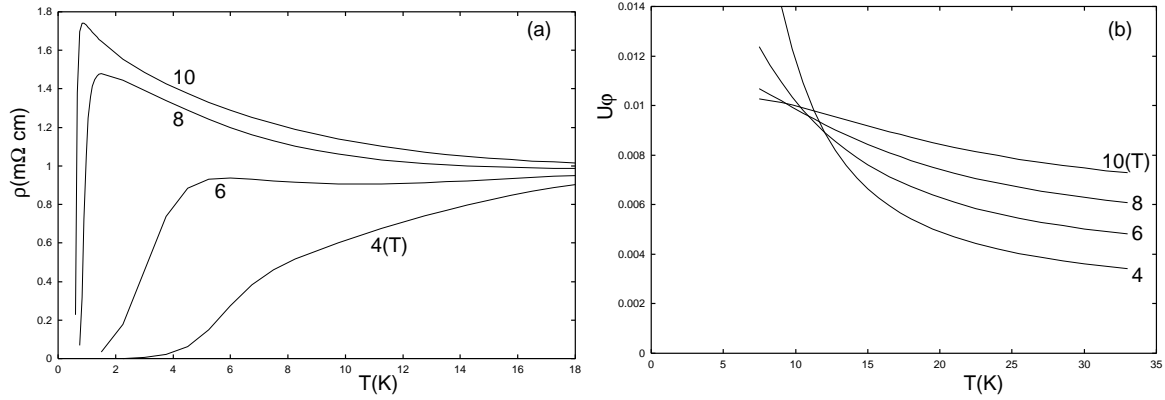
Fig. 8. (a) Resistivity curves and (b) U_ϕ-curves obtained by imagining underdoped Bi2201 data.[39] We note that $T^*_{c2}(H \leq 10(\mathrm{T})) > 8(\mathrm{K})$.

enough value of pinning strength is needed *together with* a strong quantum SC fluctuation to obtain a more remarkable FSIT behavior visible even near T_{c0}. On the other hand, the larger pinning effect enhances the VG transition field at low T. Actually, $H^*_{c2}(0)$ in Fig.8 is less than 10(T) at which a rapid drop of ρ at a finite T still occurs.

Regarding the transport energy, the U_ϕ-values in Fig.8 (b) are quite low and should be compared with other figures of U_ϕ shown in this paper. As well as the LSCO case,[20] the U_ϕ or N-values are two order of magnitude lower than a value expected by ignoring the SC pseudogap region (i.e., when $T_0 = T_{c0}$) and are consistent with the data.[39]

This comparison with underdoped Bi-2201 data corroborates the argument in ref.20 based on the LSCO data as follows. Since, in contrast to the LSCO case in $x < 0.1$, T_ν in Bi2201 seems to monotonously increase[26] with underdoping, one might expect underdoped Bi-data to behave in a qualitatively different way from the LSCO data. As seen above, however, the present theory in which T^{MF}_c corresponding to T_ν plays no essential roles explains the similarity[16, 39] in behaviors near and below T_{c0} of both ρ and U_ϕ data between Bi-2201 and LSCO. It implies that the examples of LSCO studied in ref.20 can be seen as generic behaviors of strongly underdoped cuprate materials below T_{c0}.

In this paper, the case of underdoped YBCO is not examined in details because no comparable data of ρ and N at the same doping level in underdoped YBCO have been reported. Actually, the 3D nature of SC fluctuation should be incorporated in theoretical descriptions in contrast to other cuprates which are commonly much more 2D-like, and hence, the approach in §2 may not be directly applicable to a quantitative study of doping dependences of YBCO. Nevertheless, the following features are suggested from available ρ and N data: First, the fact that, in contrast to the LSCO $x = 0.08$ data[8] showing the fan-shaped broadening below 8 (T), the ρ data in underdoped YBCO[11, 13, 47] entirely show a sharp drop implies that the enhancement of quantum fluctuation always overcomes a reduction of fluctuation upon cooling
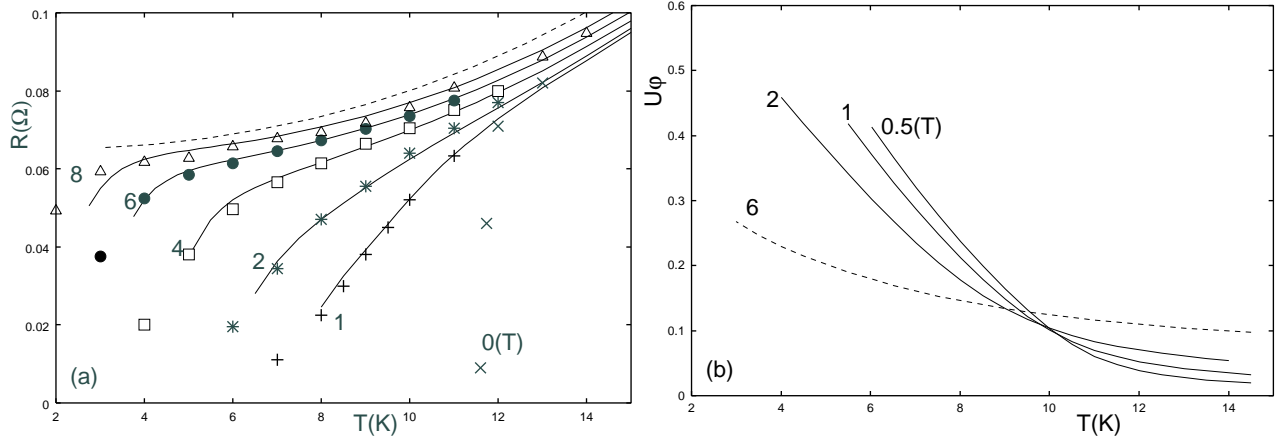
Fig. 9.   (a) Fitting results to resistivity data[18] of κ-(ET)$_2$Cu[N(CN)$_2$]Br and (b) the expected U_ϕ-
curves corresponding to the solid curves in (a). For instance, $T^*_{c2}(H = 6(T))$ lies near 8(K).

arising from a broad SC pseudogap regime, and hence, a $T_0 - T_{c0}$ value much smaller than that
in LSCO is expected. This narrower SC pseudogap regime is presumably consistent with the
Nernst coefficient[17] larger than in LSCO and Bi-2201. In any case, the doping dependences
of T_ν and T_0 in YBCO, which we expect will be remarkably different from each other, should
be clarified elsewhere.

4.   Organic Superconductors

Previously, the resistive behaviors in the vortex liquid regime of κ-(ET)$_2$ organic super-
conductors have been studied in parallel with those of cuprate materials. Typical data are seen
in refs.18 and 19. Surprisingly, the resistivity curves in κ-(ET)$_2$Cu(NCS)$_2$ with a wider vortex
liquid regime have shown a sharp drop near the irreversibility line in *all* fields shown there. In
κ-(ET)$_2$Cu[N(CN)$_2$]Br with a narrower liquid regime, the resistivity $\rho(T)$ curves have shown
a clear H-dependent crossover from the familiar fan-shaped broadening in lower H into a
sharp drop in higher H near the irreversibility line lying much below $H^*_{c2}(T)$ estimated from
the magnetization data. These features are much the same as those seen in cuprates[8, 11, 12]
and are consequences of quantum SC fluctuation becoming more important as the fluctuation
is stronger. Here, in addition to reproducing and discussing the fitting result,[25] the low T
behaviors will be examined. Numerical results in this section are also based on the use of
eqs.(23) and (24) within the framework of §2.

Resistivity data of κ-(ET)$_2$Cu[N(CN)$_2$]Br[18] are fitted in terms of the present theory, and
the results are shown in Fig.9 (a). The 3D form of σ_{vg}, eq.(17), is assumed together with $t_{\mathrm{vg}} =$
$(1 - H/H_0)^2/(1 + 3.52(H/H_0)^{1/2})$ and $c_p = 0.0035$, and the material parameters used there are
$\lambda(0) = 0.72(\mu\mathrm{m})$, $T_0 \simeq T_{c0} = 12$ (K), $H_0 = 18.3$(T), $d = 1.5$(nm), and the normal resistance
$R_n(\Omega) = 0.0574 + 0.0243\,t^{5/2}$. As a result of the large $\lambda(0)$-value, the quantum SC fluctuation
becomes essential with increasing H and leads to high field curves following $R_n(T)$ even in
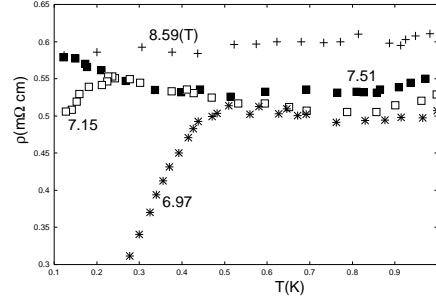
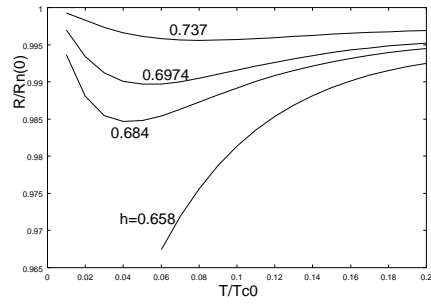Fig. 10.   Data of resistivity of κ-(ET)$_2$Cu(NCS)$_2$ near $T = 0$ and in strong fields.[49]

Fig. 11.   Resistivity curves computed for a qualitative comparison with the data in Fig.10.

$T \ll T_{c0}$. Further, the c_p-value and the t_{vg}-form suggest a much weaker pinning effect than in LSCO. For comparison, the U_ϕ curves obtained in terms of the same set of parameters are shown in Fig.9 (b). Note that, within the LLL, U_ϕ is equivalent to the magnetization, and hence that Fig.9 (b) can be also regarded as a typical example of thermodynamic quantity. A crossing behavior just below T_{c0}, which is familiar through magnetization data in many optimally-doped cuprate materials, is seen in lower fields below 2(T). It implies that the fluctuation property below 2(T) is purely thermal. In contrast, the $U_\phi(T)$-curve in 6(T) deviates from the crossing behavior in lower fields and is anomalously broadened, reflecting the stronger (quantum) fluctuation. Such an additional broadening of thermodynamic quantities due to the quantum fluctuation is an opposite trend to the corresponding behavior near $T = 0$, where a broadening of such quantities diminishes reflecting a rise of dimensionality of SC fluctuation in the quantum regime near $T = 0$.[21] This is why, as mentioned in §1, the quantum behavior at high temperatures should be distinguished from that near $T = 0$. The above features of U_ϕ seem to be consistent with the magnetization data in ref.18.

Next, the resistive behavior near $T = 0$ will be discussed based on the data of κ-(ET)$_2$Cu(NCS)$_2$ shown in Fig.10 which corresponds to Fig.3 of ref.49. In the highest field 8.59(T) above H_0 defined through a study of Shubnikov-de Haas effect,[49] $\rho(T)$ shows a T-dependence indicative of a metallic normal state and approaches a residual value $\rho_n(0)$. In lower fields just below H_0, $\rho(T)$ first decreases upon cooling as a result of thermal SC fluc-

R_n/R_Q	0.25	0.4	0.45	0.57	0.625	0.67
B_c^*/H_0	0.8	0.76	0.72	0.68	0.64	0.61
R_c/R_n	0.98	0.98	0.92	0.83	0.75	0.65

Table III. R_n/R_Q dependences of the normalized critical resistance R_c/R_n and of the normalized critical field B_c^*/H_0, estimated for each case of the calculated resistivity curves illustrated in Fig.12.

tuation, while it begins to increase on further cooling and approaches $\rho_n(0)$ (The ultimate drop of ρ due to the VG fluctuation at a low T of resistance below 7(T) will not be considered here). This insulating behavior occurs even much below H_0 and hence, is a phenomenon of a SC origin. This feature in Fig.10 is a direct evidence of an insulating behavior[21,50] arising from a purely dissipative quantum SC fluctuation in cases with metallic normal resistance. For comparison, we give in Fig.11 examples of computed $\rho(T)$ curves with such a fluctuation-induced insulating behavior at low enough T. In Fig.11, the 2D $\sigma_{\rm vg}$, eq.(18), was used, and the parameter values, $\lambda(0) = 1.1(\mu{\rm m})$, $b_p = (2\pi\xi_0^2 d)\,0.06$, $T_0 = T_{c0} = 25({\rm K})$, and $H_0 = 19({\rm T})$, were chosen. Further, the relations $(R_Q d\sigma_n)^{-1} = 0.35(1 + 0.05(T/T_{c0})^{5/2})$ and $\mu_0 = T/T_{c0} - 1 + H/H_0$ were used, and, for simplicity, the vertex correction to the pinning strength was neglected by setting $\tilde{b}_p = b_p$.

5. *s*-wave Dirty Films

In ref.23, we have proposed a theory of field-tuned superconductor-insulator (FSIT) behavior in *homogeneously* disordered thin SC films with *s*-wave pairing on the basis of a familiar electronic model in dirty limit including effects of a repulsive mutual interaction between electrons. It has been argued there how, reflecting differences in T-dependences between various components in σ, the resistance value R_c on an apparent FSIT field B_c^* and the resistive behavior around B_c^* are affected by the normalized value R_n/R_Q of the (high temperature) sheet resistance. However, no detailed computation results based on the derived GL action were given there. Motivated by a recent finding on R_c v.s. R_n relation,[51] some computed results on resistance curves consistent with the experimental observations[51,52] will be presented here. In contrast to the previous two sections, we take account of the fact that the resistance data of *s*-wave amorphous films are conventionally discussed in terms only of the R_n/R_Q value and will not try here to fit to real data. Actually, the expressions (see Appendix A) we use here for microscopic parameters were derived from the simplest extension of the BCS model to the case with both the disorder and a repulsive interaction between the electrons and may not explain quantitatively materials, for example, with a strong spin-orbit scattering.

The coefficients of each term of the GL action for the *s*-wave SC films were studied elsewhere.[53,54] In Appendix A, they will be given in a form useful for numerical computations.
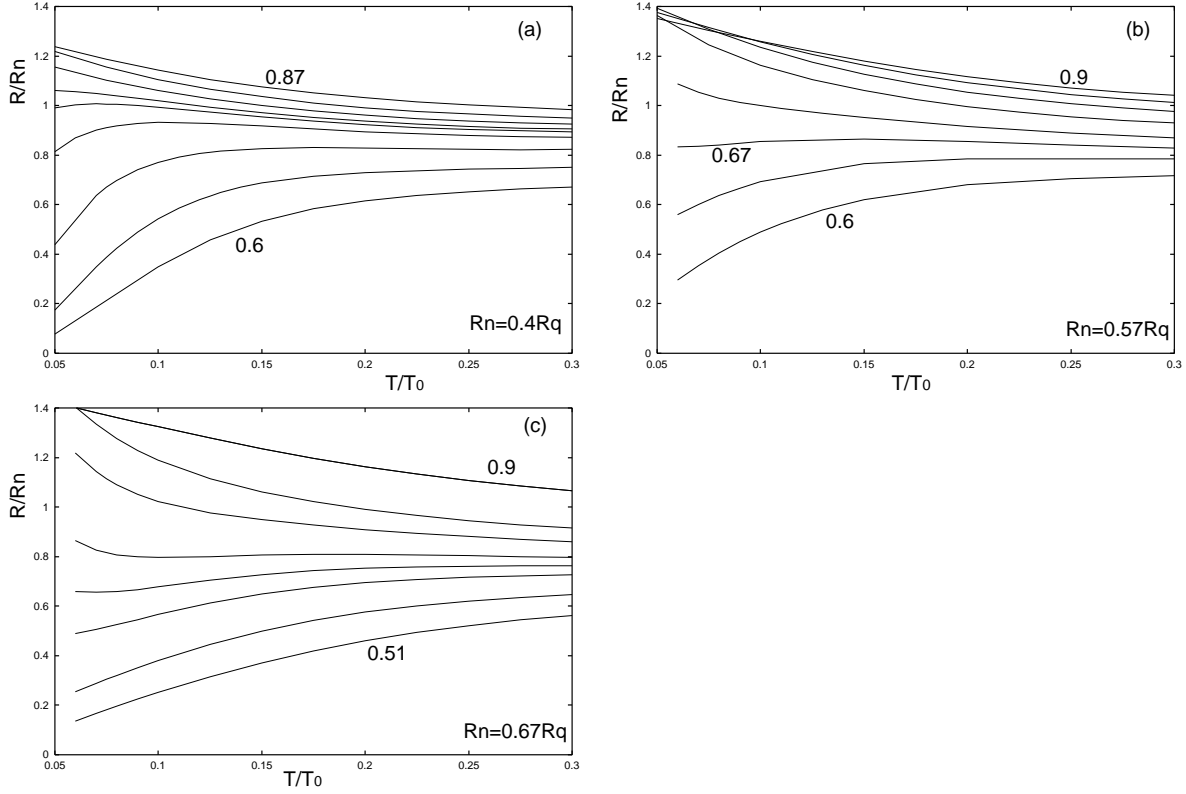
Fig. 12. Calculated resistivity curves imagining s-wave dirty films for three R_n/R_Q values : (a) $R_n/R_Q = 0.4$ in $H/H_0 = 0.87$, 0.82, 0.79, 0.77, 0.76, 0.74, 0.7, 0.65, and 0.6, (b) $R_n/R_Q = 0.57$ in $H/H_0 = 0.9$, 0.85, 0.8, 0.75, 0.7, 0.67, 0.64, and 0.6, and (c) $R_n/R_Q = 0.67$ in $H/H_0 = 0.9$, 0.8, 0.67, 0.63, 0.61, 0.59, 0.55, and 0.51.

Applying those GL coefficients to eq.(9) and using eq.(18) as $\sigma_{\rm vg}$, we have examined the resistance curves near B_c^* in details, and the results are shown in Fig.12. Since, as mentioned in Appendix A, the value of the parameter τT_0 was fixed, the normalized sheet resistance (defined at high T) R_n/R_Q is the only material parameter for our calculation of $R_Q d\sigma$ and determines *both* strengths of quantum fluctuation and vortex pinning. Let us define B_c^* as the field at which $R(T)$ takes a value R_c insensitive to T at low enough T within the examined temperature range.

From the resistance curves shown in Fig.12, one will find the following two features on the curves near B_c^*. First, for lower values of R_n/R_Q, the curves near B_c^* show an insulating T-dependence at intermediate temperatures, while they, for large R_n/R_Q values, rather decrease upon cooling in the same temperature region. This feature has been seen in various data[55–58] and justifies the scenario predicted in ref.23. At least within the present model of s-wave thin films, the decrease of $R(B_c^*)$ upon cooling for large enough R_n/R_Q-values is dominated by an enhancement of pinning strength, while its increase in smaller R_n-values occurs primarily reflecting an enhancement of quantum SC fluctuation. For instance, the insulating $R(B \simeq B_c^*)$

for $R_n = 0.4R_Q$ is controlled primarily by the quantum behavior of σ_{fl} rather than σ_{vg}. Next, as listed in Table III, R_c at lower R_n ($\leq 0.5R_Q$) values roughly coincides with R_n, while R_c in $R_n \geq 0.6$ rather decreases with increasing R_n. The relation $R_c \simeq R_n$ at low disorder (lower R_n) coincides with the experimental results in $R_n \leq 5(\mathrm{k}\Omega)$ summarized in Fig.4 of ref.52, while the saturation and reduction of R_c at higher disorder qualitatively agree with Fig.4 of ref.51.

Finally, we will comment on the validity of eq.(9) used in obtaining Fig.12 on the basis of the microscopic informations in Appendix A. When replacing eq.(4) with eq.(9), the pinning effect was underestimated. This simplification needs to be reconsidered in a close vicinity of a VG transition point (i.e., $\mu_{\mathrm{vg}} \to +0$). In trying to fit various data in §3 and 4, we did not have to discuss the details of resistivity data in the vicinity of the VG transition. In contrast, describing in details the resistive behaviors in 2D disordered thin films at low enough T and near B_c^* (i.e., near the quantum VG transition) is needed to clarify the physics of FSIT. We have partly carried out numerical computations based on eq.(4), although such a cumbersome analysis will not be presented here, and found that, roughly speaking, numerical results following from eq.(9) in the cases of R_n/R_Q-values used in Fig.12 are quantitatively unreliable only in $T/T_{c0} < 0.05$. For this reason, no data in $T/T_{c0} < 0.05$ have been shown in Fig.12.

6. Comments and Discussion

First, a view extended over a wider temperature range of the resistivity curves in Fig.12 (b) is shown in Fig.13. From this figure, a $T = 0$ 2D VG transition point B_c^* is suggested to apparently lie much below $H_{c2}^*(0)$, because B_c^* itself is lowered by the quantum SC fluctuation,[53] while the FSIT behavior appearing around B_c^* is a reflection of the VG fluctuation. Since the flat or insulating resistive behaviors appear in $H \geq B_c^*$, the temperature at which $R(T)$ in a field slightly below B_c^* drops *inevitably* lies far below $T_{c2}^*(H)$ indicated by a dark circle in the figure. Since the FSIT behavior is a consequence of strong quantum SC fluctuation, this example means that the sharp resistive drop much below $H_{c2}^*(T)$ in systems with strong quantum fluctuation is not an artifact of approximations used in calculations but a generic feature occurring commonly in clean and dirty limits irrespective of calculation methods of $R(T)$.

As shown in §3, the quantum SC fluctuation plays important roles in many cuprate materials under a high field. If the quantum SC fluctuation becomes essential, as in the example of Fig.1, due to a growth of $\lambda(0)$, one might expect the critical region of the thermal SC transition in $H = 0$ to also widen due to the $\lambda(0)$-growth. Actually, it was questioned in ref.26, through Figs.7 and 8 there, whether the pictures arguing a pseudogap of SC fluctuation origin are consistent with the fact that the critical region of the $H = 0$ transition does not widen much with underdoping. If the approach in §2 is extended to the $H = 0$ case, however, we
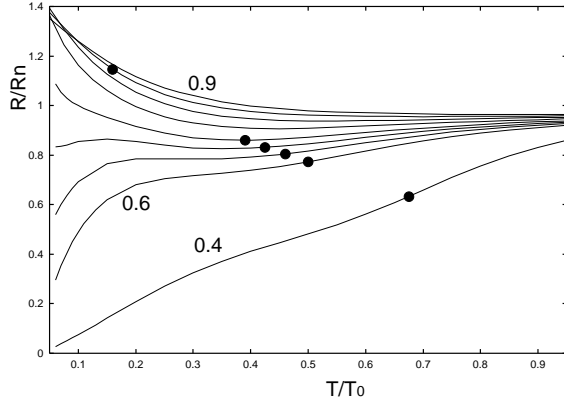
Fig. 13.   Extended view of Fig.12 (b) to higher temperatures. Here, a curve in $H = 0.4H_0$ is added further. The darked circle on each $\rho(T)$ curve denotes $T_{c2}^*(H)$ in each H.

find two theoretical facts satisfactorily explaining the sharp $H = 0$ transition in underdoped cuprates. First, it is easily noticed that the microscopic T-dependence in the broad SC pseudogap regime of the coefficient of the gradient term in GL model results in a reduction of the width of the critical region around T_{c0} in $H = 0$. Actually, by noting that this GL coefficient in $H = 0$ is nothing but that of the H-linear term in eq.(23), one easily finds that the 2D Ginzburg number *near* T_{c0} is given, *consistently* with eq.(2), by $16\pi^2[\lambda(0)]^2 k_B(T_{c0})^3/(\phi_0^2 dT_0^2)$, where the reduction factor $(T_{c0}/T_0)^2$ arises from a *microscopic* T-dependence above T_{c0} of the gradient term. Within the present approach in §2 where no specific origin leading to a reduction of the time scale γ is assumed, this may be adequate for understanding the unexpectedly narrow[26, 60] $H = 0$ critical region of underdoped cuprates. In a system with strong fluctuation, we have another mechanism of a shrinkage of the $H = 0$ critical region due to the quantum SC fluctuation itself. An explanation of this mechanism will be given in Appendix B. This mechanism is particularly effective when the enhancement of quantum SC fluctuation is primarily due to a decrease of the dissipative time scale γ. In any case, a shrinkage of the $H = 0$ critical region in a system with strong fluctuation is not a surprising phenomenon.

We need to comment here on the definition of penetration depth comparable with experimental data.[59] The actual penetration depth in $H = 0$ is defined as the mass of the gauge field through the gradient term. Then, by taking account of the T-dependence of the gradient term in the SC pseudogap regime mentioned above, the penetration depth to be observed near T_{c0} is found to be not $\lambda(0)/(1 - T/T_{c0})^{1/2}$ but $T_{c0}\lambda(0)/[T_0(1 - T/T_{c0})^{1/2}]$. If a T-dependence of the coefficient b in the SC pseudogap region can be neglected, the former is the quantity to be observed as the penetration depth in $H = 0$ and at low T where the fluctuation is negligible. Thus, in underdoped materials with wider SC pseudogap region, the $[\lambda(T)]^{-2}$ v.s. T curve is not linear even approximately, and, as observed in ref.59, the local slope $|d\lambda^{-2}/dT|$ increases on approaching T_{c0} from below. However, we note that the $\lambda(0)$-values we have es-

timated by fitting are slightly longer than those estimated experimentally.[59] If effects of the competing orders may be relatively negligible, the b-value near T_{c0} will be, as well as γ_0, larger than that near T_0. Thus, the differences between $\lambda(0)$-values obtained through Fig.6 and their experimental data[59] do not necessarily require modification of the present theory.

It should be stressed that key data[16, 17, 19, 39] showing the *uncorrelated*[20] behavior between the Nernst coefficient (or the magnetization) and the resistivity were explained in the preceding sections without taking account of electronic states peculiar to materials near a Mott transition. In the case of cuprates, such a behavior tends to arise in systems with low $H_c(0)$ such as the overdoped and underdoped materials, while it is rarely seen in optimally-doped cuprates with higher $H_c(0)$.[11, 12] This *nonmonotonic* doping dependence in the cuprates we have explained in §3 strongly suggests that the *uncorrelated* behavior is not a consequence of a strong reduction of the friction coefficient due to a microscopic mechanism[60, 61] peculiar to systems close to a Mott transition. It does not seem to us that the observation,[8, 11, 12] that the uncorrelated behavior and the sharp resistive drop are more remarkable in higher fields, while the fan-shaped broadening is usually seen in lower fields, can be explained in terms of such an approach[60, 61] based on a single vortex picture valid in low enough fields. Further, as emphasized in §1 and elsewhere,[20] the uncorrelated resistive behavior is *not* peculiar to the cuprates near a Mott transition but also appears commonly in other superconductors such as the organic materials and disordered films with an s-wave pairing (see Figs.9 and 13).

In Fig.6 (a), we have included a $\rho(T)$ curve at 29(T) which is above $H_{c2}^*(0)$ (see also Fig.8). The sharp drop of this curve near 10(K) indicates a 3D VG transition point *above* $H_{c2}^*(T)$. Since, in principle, the VG transition may occur as far as the SC fluctuation is present, such a 3D VG transition and hence, a sharp resistive drop *in* the SC pseudogap region $T_{c2}^*(H) < T < T_0(H)$ may be present, in contrast to the scenario in ref.60 for the data,[7] even in *homogeneously* disordered materials. The features seen in $(K,Ba)BiO_3$ reported in ref.62 may be a remarkable example with $T_{c2}^* < T_{vg} < T_0(H)$.

It is interesting to connect the nonmonotonic[26] doping dependence of $T_\nu(x)$ in LSCO to a sign change[63] of the fluctuation Hall conductivity $\sigma_{fl,xy}$. It is now clear[64, 65] that a sign reversal of Hall conductivity, usually seen in the vortex liquid regime, may occur above $H_{c2}^*(T)$, depending on the materials. It means that this Hall-sign reversal should be understood based on the fluctuation scenario[66] unrelated to the electronic states of vortex cores. According to this scenario, the sign of $\sigma_{fl,xy}$ is determined by that of $\partial T_c^{MF}/\partial x$, and hence, if T_ν is essentially identical with T_c^{MF}, the sign change of $\partial T_\nu/\partial x$ should appear directly as that of $\sigma_{fl,xy}$, where T_c^{MF} was defined in §3. According to ref.63, the LSCO data in $x \geq 0.12$ show a Hall-sign reversal, while available ρ_{xy} data in $x = 0.08$[67] have not shown any sign reversal, consistently with our expectation. On the other hand, according to ref.15, it appears that the Hall data of very underdoped Bi2201 still show a sign reversal, consistently with the monotonic doping

dependence of T_ν of this material.[26] This is why the identification between T_ν and T_c^{MF} seems to be consistent with available Hall-resistance data.

In hole-doped cuprates, the positive magnetoresistivity in the SC pseudogap region above T_{c0} is enhanced with underdoping. Actually, this trend has led the authors in ref.47 to argue that ξ_0 increases with underdoping. This enhanced magnetoresistivity above T_{c0} can be seen as having a common origin to the resistivity curves[16, 17, 39] following the extrapolated normal curve even much below $T_{c2}^*(H)$ ($< T_{c0}$). Actually, in a strong SC fluctuation case such that its quantum nature is no longer negligible, the Gaussian approximation for the SC fluctuation fails, and the interaction between the SC fluctuations may be important even much above T_{c0}. Hence, the quantum SC fluctuation may be a main origin of the enhanced[47] magnetoresistance in the SC pseudogap region (i.e., $T_{c0} < T < T_0$). In any case, as demonstrated in ref.20, focusing only on $\rho(T)$ data in cases with low $H_c(0)$ and hence, with large quantum fluctuation, tends to lead to an erroneous estimation of material parameters. A simultaneous study of other quantities, such as U_ϕ, measured consistently with ρ is indispensable. Further, the neglect of SC pseudogap region in thermodynamic quantities such as the magnetization[68] has also erroneously led one to concluding a ξ_0 increasing with underdoping.

During preparing this manuscript for submission, several related works[73, 74] on transport phenomena in the vortex liquid regime were reported. The *monotonic* decrease[20] of ξ_0 accompanying underdoping we have concluded through fitting to data was also argued[73] from an extrapolation of Nernst data to very higher fields in which experimental measurements cannot be performed. The uncorrelated behavior between the resistivity and the Nernst data seen in underdoped $\mathrm{Pr}_{2-x}\mathrm{Ce}_x\mathrm{CuO}_4$ was erroneously interpreted in ref.74 as an insensitivity of the resistivity to SC fluctuations. As we have clarified here, a theoretically valid explanation is provided only by noting the reduction of σ_s induced by the quantum SC fluctuation at nonzero temperatures.

Acknowledgements

Appendix A

Here, we give numerically useful expressions of the coefficients of the GL action in the case of s-wave dirty films.[23, 53, 54] In obtaining them, we are largely based on the ordinary dirty limit in quasi 2D case where the 2D diffusion and fluctuation propagators are assumed consistently with a 3D electronic state (see the second paper of ref.23), and effects of Coulomb interaction between the electrons are included perturbatively and modelled in a form interpolating between the low T/H and high T/H regions. The GL coefficients of the quadratic

term we use in §5 are given by

$$\mu_0 = \ln(T/T_0) + \sum_{n \geq 0} \frac{1}{(n+1/2)((n+1/2)\tilde{t}+1)} \tag{A·1}$$

$$+ \frac{R_n}{24\pi R_Q}(\ln(2T_0/(T+T_{cr}^{\mathrm{mf}})))^3,$$

$$(\mathcal{G}_1(0))^{-1} \simeq \mu_1 - \mu_0 \tag{A·2}$$

$$= 2\tilde{t} \sum_{n \geq 0} \frac{1}{(1+\tilde{t}(n+1/2))(3+\tilde{t}(n+1/2))},$$

and

$$\gamma_0 \simeq \gamma_1 = \gamma^{(0)}/(1 + \frac{5R_n}{8\pi R_Q}(\ln(2T_0/(T+T_{cr}^{\mathrm{mf}})))^2) \tag{A·3}$$

$$= \frac{\tilde{t}}{4\pi T_{cr}^{\mathrm{mf}}} \sum_{n \geq 0}(1+\tilde{t}(n+1/2))^{-2}$$

$$\times (1 + \frac{5R_n}{8\pi R_Q}(\ln(2T_0/(T+T_{cr}^{\mathrm{mf}})))^2)^{-1},$$

where $T_{cr}^{\mathrm{mf}} = 0.14T_0 H/H_{c2}^d(0)$, $H_{c2}^d(0)$ is H_0 in dirty limit, $\tilde{t} = T/T_{cr}^{\mathrm{mf}}$, R_n is the sheet resistance of a quasi 2D film at high T inversely proportional to the film thickness d, and γ_0 in dirty limit with no electron repulsion was denoted as $\gamma^{(0)}$. For simplicity, a SC pseudogap region is assumed to be absent (i.e., $T_0 = T_{c0}$), and $\gamma_0 = \gamma_1$ was additionally assumed because a difference between them is less important in dirty limit than that in clean limit (see eq.(23)) where γ_1 tends to vanish in $T \to 0$ limit. No interaction correction to $\mathcal{G}_1(0)$ was included because, as explained in §2 and ref.23, a detailed form of $\mathcal{G}_1(0)$ is *not* reflected in σ_{fl} and σ_{vg}.

On the other hand, the coefficients b and b_p, respectively, of the interaction and pinning terms will be expressed as

$$b = \frac{r_B^2 dR_n}{3R_Q} \frac{\tilde{t}}{T_{cr}^{\mathrm{mf}}} \sum_{n \geq 0}(1+\tilde{t}(n+1/2))^{-3}, \tag{A·4}$$

and

$$b_p = \left(\frac{r_B R_n}{R_Q}\right)^2 \frac{d\tilde{t}}{6\pi} \sum_{n \geq 0}\sum_{m \geq 0}(n+m+1)^{-1} \tag{A·5}$$

$$\times (1+\tilde{t}(n+1/2))^{-1}(1+\tilde{t}(m+1/2))^{-1}.$$

Effects of electron-repulsion on b and γ_0 were included altogether just in γ_0 since its effect on γ_0 was estimated in ref.53 to be much larger than that in b, and they usually appears as the quantum fluctuation strength $\propto b/\gamma_0$ in the quantum regime. We note that b_p is $U_p f_{00}(0)$ in the notation of ref.23. Through the computations of resistivity curves shown in Figs.12 and 13, for simplicity, another parameter $2\pi T_0 \tau$, where τ denotes the elastic scattering time, was fixed to 0.5. We expect a detailed value of this parameter not to significantly affect the

numerical results.

As a normal conductivity σ_n for this case, the expression

$$R_Q d\sigma_n = (1 - \frac{R_n}{3R_Q}\frac{2\pi r_B^2 d\gamma^{(0)}}{b}\Sigma_0)/[1 + \frac{R_n}{4\pi R_Q}\ln(T_0/T)] \tag{A·6}$$

was used in the following figures, where Σ_0 is given by eq.(10). The second term of the numerator corresponds to the low T form of additional quantum SC fluctuation contributions[69] to σ_n excluded in the GL approach and was argued[23,70] to be the origin of the *fluctuation-induced*[71] negative magnetoresistance in 2D and at low T. Such a behavior visible in higher H and lower T in Fig.12 is a consequence of this fluctuation term. Further, to represent $\ln(T_0/T)$-term in the denominator of σ_n ensuring $\sigma_n(T \to 0) \to 0$, a form of σ_n expected[72] in the case with a strong spin-orbit scattering and with long-ranged Coulomb interaction was conveniently assumed as a model. In this way, when H and T are scaled, respectively, by $H_{c2}^d(0)$ and T_0, both the GL coefficients and $R_Q d\sigma_n$ are parametrized only by R_n/R_Q.

Appendix B

Here, it will be explained how the quantum fluctuation itself reduces the width of critical region of the $H = 0$ transition at T_c. To sketch the essence of this effect, we will just treat a counterpart of eq.(4) (with $b_p = \Delta\Sigma_l = 0$) in the Hartree approximation and in $H = 0$. In the isotropic 3D case, the renormalized mass μ_R (corresponding to $[\mathcal{G}_0(0)]^{-1}$) yields the relation

$$\mu_R - \ln(T/T_c) = \sum_\omega [\zeta(\mu_R; \omega) - \zeta(0; \omega)], \tag{B·1}$$

where

$$\zeta(\mu_R; \omega) = 2\pi[\varepsilon_G^{(3)}(T)]^{1/2} \int_\mathbf{q} \frac{1}{\mu_R + q^2 + \gamma|\omega|}, \tag{B·2}$$

$\varepsilon_G^{(3)}(T) = [16\pi^2(\lambda(0))^2/(\beta\xi_0\phi_0^2)]^2$ is the 3D Ginzburg number at temperature T, and T_c was redefined so that $\mu_R(T = T_c) = 0$ is satisfied. The thermal ($\omega = 0$) part of the r.h.s. of eq.(B1) becomes $-(\varepsilon_G^{(3)}(T))^{1/2}\sqrt{\mu_R}$. If keeping only this contribution in the r.h.s. and focusing on the low μ_R limit, the critical exponent $\nu = 1$ of the correlation length in the spherical limit is obtained. On the other hand, the sum of other $\omega \neq 0$ terms in the r.h.s. is well approximated by $-\pi^{-2}\mu_R\sqrt{\varepsilon_G^{(3)}(\gamma^{-1})}$ if the quantum fluctuation is strong enough. Then, solving eq.(B1) with respect to μ_R, one finds the width of critical region to be estimated as $T_c\varepsilon_G^{(3)}(T_c)/[16(1 + \pi^{-2}\sqrt{\varepsilon_G^{(3)}(\gamma^{-1})})]$, implying that, with decreasing γ, the critical region is narrower. The basic reason of this narrowing of the critical region due to the quantum fluctuation consists in the fact that the width of quantum critical region at $T = 0$ and in 3D is negligible, because the dimensionality of the dissipative quantum critical fluctuation at $T = 0$ in D-dimension is $D + 2$, which is above the upper critical dimension (i.e., four) for $D > 2$.[75]

References

1) R. Ikeda, T. Ohmi and T. Tsuneto: J. Phys. Soc. Jpn. **60** (1991) 1051.

2) R. Ikeda, T. Ohmi and T. Tsuneto: Phys. Rev. Lett. **67** (1991) 3874.

3) S. Sarti, D. Neri, E. Silva, R. Fastampa and M. Giura: Phys. Rev. **B** 56 (1997) 2356.

4) R. Ikeda: J. Phys. Soc. Jpn. **70** (2001) 219.

5) D. S. Fisher, M. P. A. Fisher and D. A. Huse: Phys. Rev. B **43** (1991) 130.

6) T. Nattermann and S. Sheidl: Adv. Phys. **49** (2000) 607.

7) A. P. Mackenzie, S.R. Julian, G.G. Lonzarich, A. Carrington, S.D. Hughes, R.S. Liu and D.C. Sinclair: Phys. Rev. Lett. **71** (1993) 1238.

8) M. Suzuki and M. Hikita: Phys. Rev. B **44** (1991) 249.

9) A. Carrington, A. P. Mackenzie and A. Tyler: Phys. Rev. B **54** (1997) R3788.

10) S. Kleefisch, B. Welter, A. Marx, L. Alff, R. Gross and M. Naito: Phys. Rev. B **63** (2001) 100507; F. Gollnik and M. Naito: Phys. Rev. B **58** (1998) 11734.

11) D. J. C. Walker, O. Laborde, A.P. Mackenzie, S.R. Julian, A. Carrington, J.W. Loram and J.R. Cooper: Phys. Rev. B **51** (1995) 9375.

12) A. Carrington, A.P. Mackenzie, D.C. Sinclair and J.R. Cooper: Phys. Rev. B **49** (1994) 13243.

13) V. F. Gantmakher, G.E. Tsydynzhapov, L.P. Kozeeva and A.N. Lavrov: JETP **88** (1999) 148.

14) K. Karpinska, A. Malinowski, M.Z. Cieplak, S. Guha, S. Gershman, G. Kotliar, T. Skoskiewicz, W. Plesiewicz, M.Berkowski and P. Lindenfeld: Phys. Rev. Lett. **77** (1996) 3033.

15) S. I. Vedeneev, A.G.M. Jansen, E. Haanappel and P. Wyder: Phys. Rev. B **60** (1999) 12467.

16) C. Capan, K.Behnia, J.Hinderer, A.G.M. Jansen, W. Lang, C. Marcenat, C. Marin and J. Flouquet: Phys. Rev. Lett. **88** (2002) 056601.

17) Y. Wang, N.P. Ong, Z.A. Xu, T. Kakeshita, S. Uchida, D.A. Bonn, R. Liang and W.N. Hardy: Phys. Rev. Lett. **88** (2002) 257003.

18) T. Sasaki et al.: unpublished. See also A. Matsuyama, T. Sasaki, T. Fukase and N. Toyota: Physica C **263** (1996) 534.

19) H. Ito, T. Ishiguro, T. Komatsu, G. Saito and H. Anzai: Physica B **201** (1994) 470.

20) R. Ikeda: Phys. Rev. B **66** (2002) 100511(R).

21) R. Ikeda: Int. J. Mod. Phys. B **10** (1996) 601.

22) H. C. Ri, R. Gross, F. Gollnik, A. Beck, R.P. Huebener, P. Wagner and H. Adrian: Phys. Rev. B **50** (1994) 3312.

23) H. Ishida and R. Ikeda: J. Phys. Soc. Jpn. **71** (2002) 254 and (2002) 2352.

24) G. Blatter and B. Ivlev: Phys. Rev. Lett. **70** (1993) 2621.

25) R. Ikeda: Physica B **329-333** (2003) 1457.

26) Y. Wang, Z.A. Xu, T. Kakeshita, S. Uchida, S. Ono, Y. Ando and N.P. Ong: Phys. Rev. B **64** (2001) 224519.

27) D. R. Niven and R. A. Smith: Phys. Rev. B **66** (2002) 214505.

28) O. Vafek, A. Melikyan and Z. Tesanovic: Phys. Rev. B **64** (2001) 224508.

29) K. Izawa, A.Shibata, H.Takahashi, Y.Matsuda, M.Hasegawa, N.Chikumoto, C.J. van der Beek and M. Konczykowski: J. Low Temp. Phys. **117** (1999) 1193; Y. Matsuda, A. Shibata, K. Izawa, H. Ikuta, M. Hasegawa and Y. Kato: Phys. Rev. B **66** (2002) 014527.

30) S. Ullah and A. T. Dorsey: Phys. Rev. B **44** (1991) 262.

31) See, for instance, T. R. Kirkpatrick and D. Belitz: Phys. Rev. Lett. **79** (1997) 3042.

32) R. Ikeda: J. Phys. Soc. Jpn. **64** (1995) 1683.

33) B. I. Halperin and D. R. Nelson: J. Low Temp. Phys. **36** (1979) 599. The temperature T_c^0 in this reference corresponds to T_{c0} in the present paper.

34) R. J. Troy and A. T. Dorsey: Phys. Rev. B **47** (1993) 2715.

35) C-R. Hu: Phys. Rev. B **13** (1976) 4780 and references therein.

36) R. Ikeda: J. Phys. Soc. Jpn. **66** (1997) 1603.

37) In contrast to a specific case (see Ref.23) of s-wave dirty films, the critical VG conductance value is *always* nonuniversal in general case where the parameters γ_0, b_p, and b are independent of each other.

38) P. W. Anderson: J. Phys. Chem. Solids **11** (1959) 26.

39) C. Capan, K. Behnia, Z. Z. Li, H. Raffy and C. Marin: Phys. Rev. B **67** (2003) 100507(R).

40) See, for instance, P. A. Lee and M. G. Payne: Phys. Rev. B **5**(1972) 923.

41) Strictly speaking, the lower limit 0 of the s-integral in the μ_n-expression should be replaced by T/ω_c, where ω_c is a high energy cutoff. The numerical $\rho(T)$ curves shown in the figures were unaffected by the choice of this lower limit in the T/T_0 ranges where we have numerically examined.

42) Although, in the $d_{x^2-y^2}$-pairing, cross terms between the lowest LL and the $n = 4m$ $(m \geq 1)$ higher LLs arise in the quadratic terms of eq.(2.1) so that the derivation of eq.(3.2) may be affected, the higher LLs can be safely neglected unless $H/H_{c2}^*(0) \ll 1$.

43) V. F. Mitrovic, H.N. Bachman, W.P. Halperin, A.P. Reyes, P. Kuhns and W.G. Moulton: Phys. Rev. B **66** (2002) 014511.

44) B. Khaykovich, Y.S. Lee, R.W. Erwin, S.-H. Lee, S. Wakimoto, K.J. Thomas, M.A. Kastner and R.J. Birgeneau: Phys. Rev. B **66** (2002) 014528.

45) S. A. Kivelson, D.-H. Lee, E. Fradkin and V. Oganesyan: Phys. Rev. B **66** (2002) 144516.

46) E. Demler, S. Sachdev and Y. Zhang: Phys. Rev. Lett. **87** (2001) 067202.

47) Y. Ando and K. Segawa: Phys. Rev. Lett. **88** (2002) 167005.

48) J. W. Loram, K. A. Mirza, J.R. Cooper and J.L. Tallon: Physica C **282-287**, 1405 (1997); N. Momono, T. Matsuzaki, M. Oda and M. Ido: J. Phys. Soc. Jpn. **71** (2002) 2832.

49) T. Sasaki, T. Fukuda, T. Nishizaki, T. Fujita, N. Yoneyama, N. Kobayashi and W. Biberacher: Phys. Rev. B **66** (2002) 224513.

50) R. Ikeda: J. Phys.Soc.Jpn. **65** (1996) 33.

51) E. Bielejec and W. Wu: Phys. Rev. Lett. **88** (2002) 206802.

52) P. Phillips and D. Dalidovich: Phil. Mag. **81** (2001) 847.

53) H. Ishida, H. Adachi and R. Ikeda: J. Phys. Soc. Jpn. **71** (2002) 245.

54) H. Ishida and R. Ikeda: J. Phys. Soc. Jpn. **67** (1998) 983.

55) A. F. Hebard and M. A. Paalanen: Phys. Rev. Lett. **65** (1990) 927.

56) J. A. Chervenak and J. M. Valles, Jr.: Phys. Rev. B **61** (2000) R9245.

57) V. F. Gantmakher, M.V. Golubkov, V.T. Dolgopolov, G.E. Tsydynzhapov and A.A. Shashkin: JETP Lett. **71** (2000) 160.

58) N. Markovic, C. Christiansen, A.M. Mack, W.H. Huber and A.M. Goldman: Phys. Rev. B **60** (1999) 4320.

59) C. Panagopoulos, B.D. Rainford, J.R. Cooper, W. Lo, J.L. Tallon, J.W. Loram, J. Betouras, Y.S.

Wang and C.W. Chu: Phys. Rev. B **60** (1999) 14617.

60) V. B. Geshkenbein, L. B. Ioffe and A. J. Millis: Phys. Rev. Lett. **80** (1998) 5778.

61) P. A. Lee and G. Sha: cond-mat/0209572.

62) C.Marcenat, S.Blanchard, J.Marcus, L.M.Paulius, C.J.van der Beek, M.Konczykowski and T. Klein: Phys. Rev. Lett. **90** (2003) 037004.

63) T. Nagaoka, Y. Matsuda, H. Obara, A. Sawa, T. Terashima, I. Chong, M. Takano and M. Suzuki: Phys. Rev. Lett. **80** (1998) 3594.

64) N. Kokubo, J. Aarts and P. H. Kes: Phys. Rev. B **64** (2001) 014507.

65) R. Jin and H. R. Ott: Phys. Rev. B **53** (1996) 9406.

66) R. Ikeda: Physica C **316** (1999) 189. See the footnote of the first page there.

67) W. Lang: private communication.

68) M. Li, C. J. van der Beek, M. Konczykowski, A.A. Menovsky and P.H. Kes: Phys. Rev. B **66** (2002) 024502.

69) V. M. Galitski and A. I. Larkin: Phys. Rev. B **63** (2001) 174506.

70) R. Ikeda: Phys. Rev. Lett. **89** (2002) 109703.

71) S. Okuma, S. Shinozaki and M. Morita: Phys. Rev. B **63** (2001) 054523.

72) P. A. Lee and T. V. Ramakrishnan: Rev. Mod. Phys.**57** (1985) 287.

73) Y. Wang, S. Ono, Y. Onose, G. Gu, Y. Ando, Y. Tokura, S. Uchida and N. P. Ong: Science **299** (2003) 86.

74) H. Balci, C. P. Hill, M. M. Qazilbash and R. L. Greene: cond-mat/0303469.

75) For instance, see A. J. Millis: Phys. Rev. B **48** (1993) 7183.